New Approaches for Nonlinear Acoustic Echo Cancellation

Jing Fu

A Thesis

in

The Department

of

Electrical and Computer Engineering

Presented in Partial Fulfillment of the Requirements
for the Degree of Master of Applied Science (Electrical and Computer Engineering) at
Concordia University
Montreal, Quebec, Canada

December 2007

Your file Votre référence
ISBN: 978-0-494-40881-0
Our file Notre référence
ISBN: 978-0-494-40881-0

ABSTRACT

New Approaches for Nonlinear Acoustic Echo Cancellation

Jing Fu

The nonlinearity of amplifier and/or loudspeaker gives rise to nonlinear echo in acoustic systems, which degrades seriously the performance of speech and audio communications. Many acoustic echo cancellation (AEC) schemes have been proposed by researchers to cancel the disturbing echo. In this thesis, two approaches for nonlinear echo cancellation, namely, the 2^{nd} order Volterra filter-based canceller and the sigmoid-transform-based (STB) canceller, are developed.

Volterra filter (VF) plays a critical role in modeling a nonlinear acoustic system where the nonlinear distortion is mainly caused by a loudspeaker. However, the large number of coefficients and the high computational complexity always make the VF difficult to be used in practice. By analyzing a general 2^{nd} order VF model and a cascade model consisting of a 2^{nd} order VF and a transversal filter, this thesis proposes a simplified 2^{nd} order VF structure with relatively low computational complexity for the echo canceller, which is shown to be more efficient in acoustic echo cancellation applications. A theoretically justification is also provided to show the feasibility of such a simplification. Moreover, a normalized least mean square (NLMS) algorithm for kernel-separated 2^{nd} order VF is derived to accelerate the convergence speed of the coefficients of the nonlinear filter. This algorithm uses a new range of the step size or called convergence

factor to ensure the stability of the adaptive filter. The outstanding performance of the proposed AEC is verified by computer simulations

For solving the nonlinear distortion caused mainly by an amplifier, a simple yet efficient nonlinear echo cancellation scheme is proposed by using an adaptable sigmoid function in conjunction with a conventional transversal adaptive filter. The new scheme uses the least mean square (LMS) algorithm to update the sigmoid function and the recursive least square (RLS) algorithm to determine the weight vector of the transversal filter. The proposed acoustic echo canceller is proved to be convergent under some reasonable assumptions. Extensive computer simulations show that the proposed AEC has a very satisfactory echo cancellation performance for saturation-type nonlinear distortion.

Acknowledgements

I would like to thank my supervisor, Dr. Weiping Zhu, for his guidance and technical suggestions. His time, effort and patience are much appreciated.

I am also grateful to my parents for their love, encouragement and support.

Table of Contents

List of Figures

List of Tables

List of Abbreviations

AEC	:	Acoustic Echo Cancellation
AECs	:	Acoustic echo cancellers
ERLE	:	Error Return Loss Enhancement
LMS	:	Least Mean Square
NLMS	:	Normalized Least Mean Square
RLS	:	Recursive Least Square
SD	:	Steepest Decent
STB	:	Sigmoid-Transform-Based
VF	:	Volterra Filter
WSS	:	Wide-sense stationary

List of Symbols

$\mathbf{I}$	:	Identity matrix
$J(n)$	:	Cost function
$\mathbf{p}$	:	Cross-correlation vector
$\mathbf{P}_D(n)$	:	Deterministic cross-correlation vector
$\mathbf{R}$	:	Correlation matrix
$\mathbf{R}_D(n)$	:	Deterministic correlation matrix
tr	:	Trace of a matrix
$\mathbf{w}_0$	:	Wiener solution
μ	:	Convergence factor or step size
$\sum$	:	Summation
$\|\bullet\|$	:	Euclidean norm
$(\bullet)$	:	Combination operation

Chapter 1 Introduction

In general terms echo is the repetition of a wave due to mismatch in the design of the circuitry and due to reflection from the surroundings [1]. The echo degrades the voice quality during a conversation in wired and wireless phones. There are mainly two kinds of echo, hybrid echo and acoustic echo.

Hybrid echo: this type of echo is mainly encountered in telephone lines due to impedance mismatch on the connecting lines.

Acoustic echo: an acoustic echo is produced due to the reflection from the surrounding objects in the room during a conference call or objects in a car when the wireless handset is being used. The echo produced in this manner is known as room acoustic echo.

For getting rid of the disturbance of the echo, the idea of echo cancellation used in telecommunications field began in July 1962. At very beginning, the applications of the echo cancellation were mainly focused on solving the hybrid echo problems. Later, there has been considerable interest in acoustic echo cancellers for teleconferencing. In this application, the echo is generated acoustically by the coupling between the loudspeaker and microphone through the impulse response of a conference room. In principle, the problem is similar to that of network echo cancellers, but there are some differences in

practice because the impulse responses in the acoustic case are much longer and more variable [2].

Acoustic echo cancellation (AEC) is an effective technique to suppress the echo effect and improve the communication system performance. Most AEC techniques do not consider the nonlinear distortion caused by a loudspeaker/amplifier. However, recently, it has been found that the AEC system performance could be greatly improved by considering the nonlinearities existing in the system. In most cases the implementation of the nonlinear filter is computationally expensive, owing to the large number of coefficients required to identify the nonlinear system. The high computational complexity filters may cost a lot of calculating operations and time to converge. Considering the acoustic echo cancellation is a real-time implementation, low-complexity nonlinear AECs turn out to be important. Many different nonlinear AECs have been proposed in recent years, but it is still difficult to find a practical unified model that efficiently adapts all the possible nonlinear distortions. Therefore, the performance of a nonlinear acoustic echo canceller highly depends on the nature of the echo path. The objective of this thesis is to develop two different low-complexity nonlinear models to identify two kinds of common nonlinear distortions happening in a loudspeaker/amplifier system.

1.1 Acoustic Echo

When the sound from a loudspeaker or the earpiece of a telephone handset is picked up by the microphone in the same room or the microphone in the very same handset, an acoustic echo arises and is delivered to the far-end user/speaker. This disturbance exists in all communications scenarios where the speaker and the microphone are in close distance. Examples of acoustic echo are found in everyday surroundings such as:

- A standard telephone in speakerphone or hands-free mode
- Telephone conference such as polycom's soundstation
- Hands-free car phone systems
- In-room sound systems using ceiling speakers and desk phones
- Physical coupling (vibrations of the loudspeaker transferred to the microphone via the handset casing)

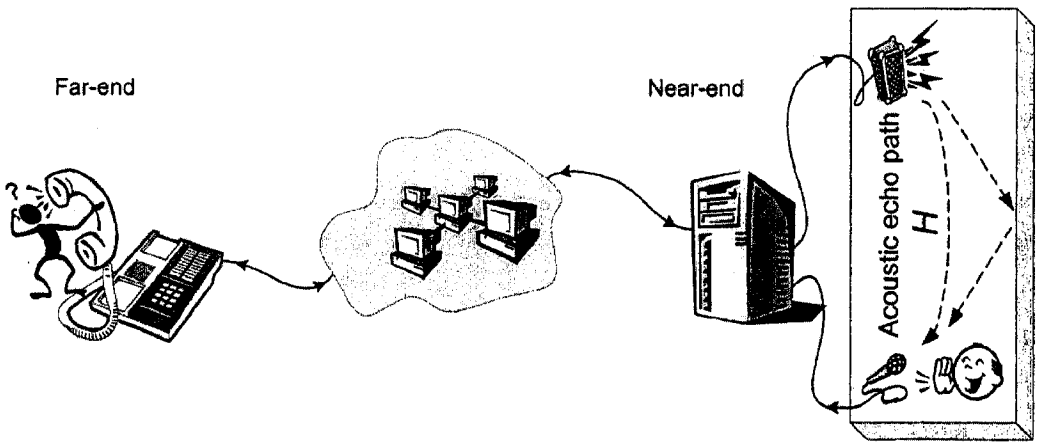

Figure 1.1 Acoustic echo produced in hands-free system

In most of these cases, the signal from the loudspeaker passes through the room and enters the microphone, which creates the so-called acoustic echo path. The acoustic echo can easily perceived by the far-end speakers in a communications conversation, as shown in Figure 1.1 [3]. Although it is attenuated in amplitude and delayed in time, it is still very disturbing to the speaker. Therefore it is of crucial importance to cancel acoustic echo. The difficulties in cancelling the acoustic echo signal stem from the alteration or the distortion of the original sound caused by the acoustic echo path. This distortion may be linear or nonlinear depending on the nature of the echo path. The echo path from the speaker to the microphone in the same room is usually characterized by a liner FIR filter. Accordingly, the echo signal arrives at the microphone is often measured by the room impulse response,

namely, the impulse response of the FIR filter. Therefore, this echo is considered to be linear. In recent years, however, researchers have found that it is not sufficient to treat the echo path as a linear system since the room impulse response does not take into account the possible nonlinear distortion caused by the loudspeaker and/or amplifier. As shown in the next section, in order to realize a high-quality voice communication, the nonlinear echo component has to be eliminated or alleviated.

1.2 Nonlinear Distortion in Loudspeaker/Amplifier

Figure 1.2 shows a complete echo path from the D/A converter in the speaker up to the A/D converter in the microphone [4]. Let us neglect in this thesis the nonlinear quantization which might be used in the D/A and A/D converters.

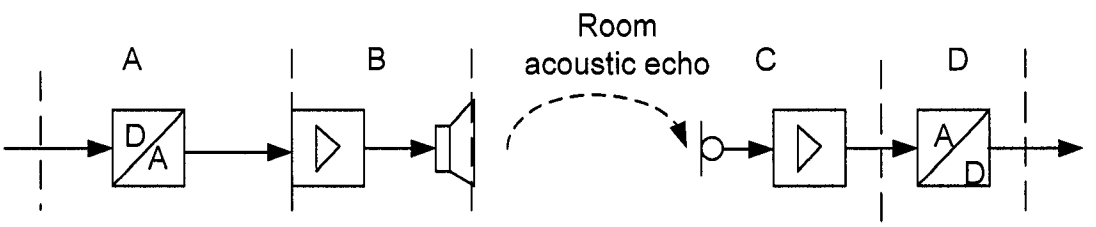

Figure 1.2 Nonlinear echo path

The main source of nonlinearity is found in part B, since the loudspeaker and the power amplifier are operated at the high signal level in the transmission chain. This part of the system is considered to be weakly time-variant, e.g. due to temperature drift. Part C consists of the room impulse response and the microphone. It is assumed to be an LTI system due to the fact that the signal received by the microphone is of low amplitude. Therefore, the nonlinear characteristic of the loudspeaker and the amplifier become critical in the cancellation of the entire acoustic echo. Previous works have discussed that the

loudspeaker and the amplifier may exhibit different nonlinear characteristics [5], [6], [7], [8].

As far as a loudspeaker is concerned, the large signal behaviour of an electrodynamic loudspeaker can be modeled by a pair of simplified nonlinear differential equations [5]:

$$u = R_e + \frac{d(L(x)i)}{dt} + Bl(x)v \tag{1.1}$$

$$Bl(x)i = ma + Rv + k(x)x - \frac{1}{2}\frac{dL(x)}{dx}i^2 \tag{1.2}$$

where u denotes the loudspeaker diaphragm velocity. The main electrical pieces are the voice-coil electrical resistance R_e and the voice-coil nonlinear self inductance $L(x)$. In equation (1.2), $Bl(x)$ is the nonlinear force factor, m represents a moving mass, R a mechanical damping and $k(x)$ a nonlinear stiffness. In spite of constructional improvements, loudspeakers still exhibit nonlinear behaviour. The main resources of nonlinearities can be summarized below [6]

- The force factor as a function of the voice coil excursion.
- The electric self-inductance depending on the voice coil excursion
- The nonlinear suspension stiffness

In some situations, the nonlinear distortion is mainly caused by an overdriven amplifier. This kind of nonlinearity can be described by a nonlinear function [7], [8], which implies that each input value is mapped to a unique output value. This kind of nonlinearity is also called memoryless nonlinearity, which especially happens in mobile equipment, where the low weight constraint requires low supply voltages.

1.3 Acoustic Echo Cancellation (AEC)

This thesis emphasizes on the cancellation of the distortion caused by the loudspeaker/amplifier and the room acoustic echo.

1.3.1 Acoustic Echo Cancellation (AEC) System

As shown in Figure 1.3, in general, an Acoustic Echo Canceller works as follows:

- The electronic sound signal received by the speaker.
- The received signal passes through the entire echo path including the nonlinear distortion and the room impulse response.
- The microphone picks up the echo which is the delayed and distorted version of the received sound signal.
- The electronic signal from the microphone is also sampled and then compared with the reference signal.
- An adaptive filter is properly designed such that the reference signal can match the echo but with 180^0 phase difference.
- If the echo is perfectly cancelled, then only the voice of the local speaker is transmitted to the far-end user.

In reality, however, a small error signal that is the difference of the reference signal and the echo still exists but it is negligible and very often not sensible by the far-end user.

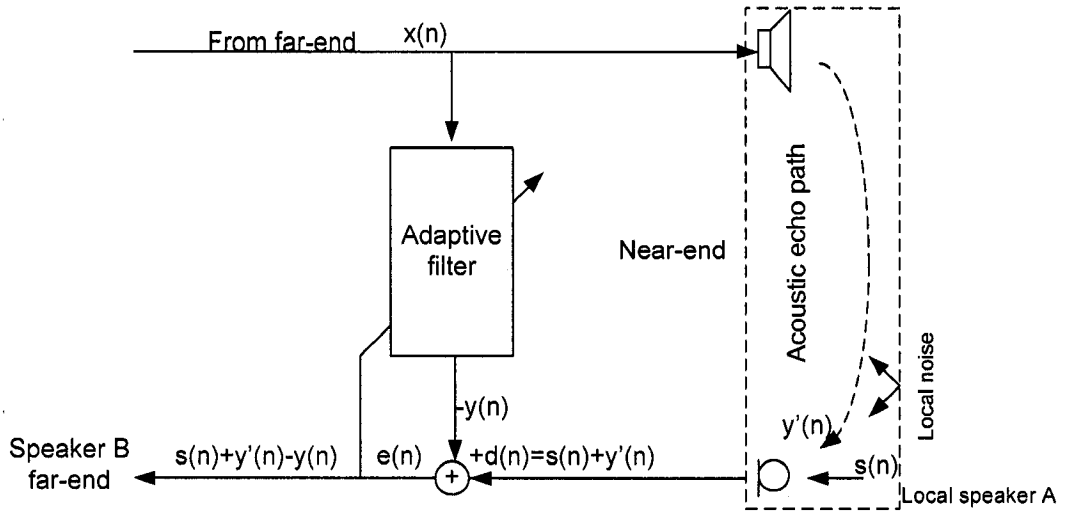

Figure 1.3 General block diagram of an acoustic echo canceller

From the above process, the residual error signal can be formulated as

$$e(n) = y'(n) - y(n) \tag{1.3}$$

Considering the signal $s(n)$ from the local speaker, the signal transmitted to the far end is given by

$$u(n) = s(n) + e(n) \tag{1.4}$$

Clearly, when $y(n)$ is equal to $y'(n)$ the signal received by the far-end user B contains only the speech from the local speaker A [9]. The error signal plays a very important role in adaptive AECs. It is used to update the weight vector, namely, the coefficient vector of the adaptive filter such that a norm of the error function is minimized. It should be noted that the adaptive filter could be linear or nonlinear. If only the linear echo is considered, a transversal filter is often used. Otherwise, if the echo is nonlinear or contains nonlinear components, using a linear adaptive filter is not sufficient. A more efficient nonlinear filter must be pursued.

1.3.2 General Requirements for AEC

Typically, an echo canceller should meet the following requirements [9]:

- Rapid convergence speed: the echo canceller should have a fast convergence speed so that it can identify and track rapidly the changes in the unknown echo path. The convergence rate depends on the adaptive algorithm as well as the structure of the adaptive filter used in the AEC.
- Accurate double talk detection: when the two speakers talk simultaneously, the echo canceller should be able to detect this double talk condition accurately. The adaptation process should then be stopped to avoid divergence of adaptive filter coefficients and cancellation of the speech signal itself. Since in real applications both sides of the communication seldom talk at the same time, we only discuss the single talk situation in this thesis.
- Low complexity: in acoustic echo cancellation, the adaptive filter needs to proceed with a large number of coefficients. This makes the implementation of complex adaptive algorithms more difficult. Therefore, it is always preferable to develop low-complexity algorithms and filter structures.
- High echo return loss enhancement (ERLE): in adaptive echo cancellation, a term known as ERLE is used to measure the effectiveness of an echo cancellation method. If this value is high, the echo canceller is considered to be good. It has been observed that the ERLE value is normally with 30dB due to the nature of the speech signals and other constraints [1], [10].

1.4 Main Contributions

This thesis studies the performance of different nonlinear AEC filters in different nonlinear acoustic echo path situations. Since each nonlinear canceller has its own advantages, we focus on the performances of a simplified 2^{nd} order VF and a saturation-curve-based nonlinear filter for AEC applications. The main contributions of this thesis are summarized as follows:

The feasibility of simplifying a 2^{nd} order VF to fit a cascade structure of nonlinear echo path without sacrificing its performance is first investigated. Since the input signal variance has a great impact on the convergence rate of the 2^{nd} order VF, a NLMS algorithm with a new range of the step size is proposed for the kernel-separated 2^{nd} order VF to reduce the effect of the input signal variance. This algorithm updates both linear and the 2^{nd} order kernels of the nonlinear filter separately, and outperforms a conventional NLMS algorithm. It is verified by computer simulations that the simplified VF structure can reduce the computational complexity of a 2^{nd} order VF significantly, while the proposed NLMS algorithm can efficiently reduce the negative effect of the input signal variance.

Considering that the saturation-type distortion is also a typical one in loudspeaker/amplifier systems, we present a new nonlinear echo canceller that uses a sigmoid function followed by a conventional linear adaptive filter, in which the parameters of the sigmoid function and the coefficients of the linear transversal filter are updated, respectively, with the LMS and RLS algorithms. A theoretical analysis of the convergence of the nonlinear transform-based acoustic echo canceller is also given.

1.5 Thesis Organization

This thesis is organized as follows:

Chapter 2 introduces the basic knowledge of linear adaptive filtering and some popular updating algorithms which can be used in nonlinear AECs.

Chapter 3 describes some previous works about nonlinear adaptive filters applied in acoustic echo cancellation. The basic structures of a VF, a cascade nonlinear filter and a nonlinear transform-based filter are introduced.

Chapter 4 focuses on the development of the 2^{nd} order VF-based techniques for acoustic echo cancellation. A simplification strategy for the 2^{nd} order VF used in AEC is proposed along with a new NLMS algorithm for the update of filter coefficients.

Chapter 5 proposes a nonlinear saturation-curve-based canceller structure consisting of a sigmoid function and an FIR filter. The convergence analysis of the nonlinear structure is also conducted, yielding a low complexity and fast convergent nonlinear acoustic echo canceller.

Chapter 6 summarizes the work completed in this thesis and provides some suggestions for future research.

Chapter 2 Linear Adaptive Filters and Applications in AEC

In this chapter, basic adaptive filtering techniques are introduced. The optimum solution for a linear filter response is derived based on some commonly used adaptation algorithms that will be adopted in the next several chapters.

2.1 Adaptive Filtering Techniques

In many applications the characteristic of a system of interest is unknown. Adaptive signal processing is a technique where an adjustable model can be designed through an iterative procedure such that the characteristic of this model best fits the unknown system. This model is termed as adaptive filter which is time-varying in natures, and normally can adjust itself according to the changes in the unknown system.

The configuration of a general adaptive system is shown in Figure 2.1. It consists of the following blocks [9]:

- Unknown system: it contains time-varying parameters depending on the type of application.
- Adaptive filter: its performance depends on the filter structure as well as the update mechanism. It is also associated with the unknown system. The input signal is passed though this filter to produce an output and form an error signal which is

used to dictate the update algorithm. Depending on application needs, this filter can be linear or nonlinear.

- Update mechanism: this is the core of an adaptive algorithm which determines the characteristics of the adaptive filter based on the performance requirement as well as the nature of the unknown system. It usually involves a set of mathematical expressions required to determine and update. These update formulas are usually derived from a minimization problem with respect to the error signal e(n). The most commonly used adaptive algorithms include the least-mean square (LMS), normalized least-mean square (NLMS), and recursive least square (RLS), etc.

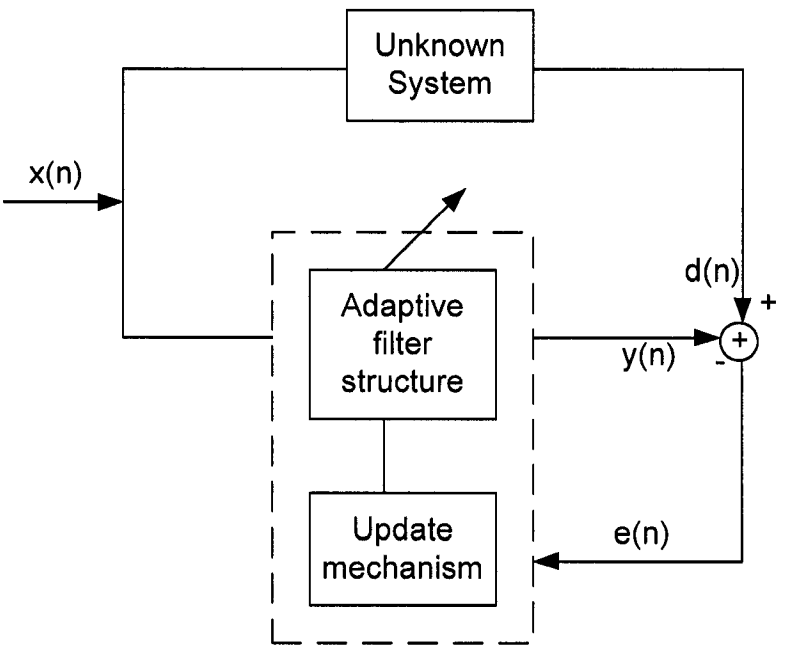

Figure 2.1 General Block Diagram of an adaptive system

Adaptive filters can be applied into many applications, including system identification, channel equalization, adaptive beamforming, signal enhancement, noise cancellation and echo cancellation. This thesis will focus on the system identification and

acoustic echo cancellation. A detailed description of the other applications can be found in [11].

Linear adaptive filter is widely used in acoustic echo cancellation (AEC) and many other fields due to its good properties such as global convergence and guaranteed stability. Many linear adaptive filtering techniques can be directly applied to nonlinear filter. In the following subsections, we review some of these techniques with an emphasis on their applications in acoustic echo cancellation. This serves as a background material for further study of nonlinear filtering algorithms in the next chapter.

2.2 Wiener Filter

One of the most widely used objective functions in adaptive filtering is the mean-square error (MSE) defined as [12]

$$E[e^2(n)] = E[(d(n) - y(n))^2] \tag{2.1}$$

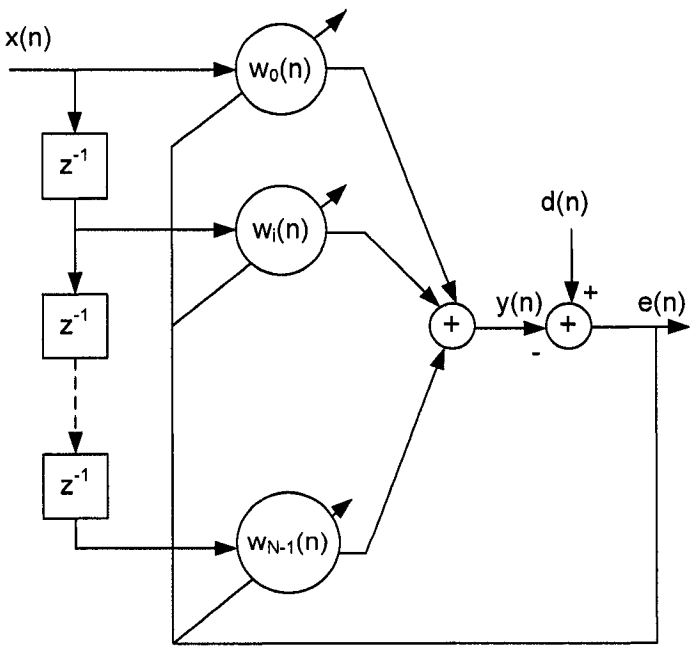

Figure 2.2 Adaptive FIR filter

A straightforward realization of the adaptive filter is to use a direct form FIR structure as illustrated in Figure 2.2, which is also called transversal filter. The output of this variable-tap FIR filter can be written as

$$y(n) = \sum_{i=0}^{N-1} w_i(n)x(n-i) = \mathbf{w}^T(n)\mathbf{x}(n) \tag{2.2}$$

where $\mathbf{x}(n) = [x(n), x(n-1), \cdots, x(n-N+1)]^T$ and $\mathbf{w}(n) = [w_0(n), w_1(n), \cdots, w_{N-1}(n)]^T$ are the input and the weight vector or coefficient vector of the filter, respectively. Using equation (2.2), the objective function (2.1) can be rewritten as

$$\begin{aligned} E[e^2(n)] = \xi(n) &= E[d^2(n) - 2d(n)\mathbf{w}^T(n)\mathbf{x}(n) + \mathbf{w}^T(n)\mathbf{x}(n)\mathbf{x}^T(n)\mathbf{w}(n)] \\ &= E[d^2(n)] - 2E[d(n)\mathbf{w}^T(n)\mathbf{x}(n)] + E[\mathbf{w}^T(n)\mathbf{x}(n)\mathbf{x}^T(n)\mathbf{w}(n)] \end{aligned} \tag{2.3}$$

For a filter with fixed coefficients, the MSE function is given by

$$\xi = E[d^2(n)] - 2\mathbf{w}^T\mathbf{p} + \mathbf{w}^T\mathbf{R}\mathbf{w} \tag{2.4}$$

where $\mathbf{p} = E[d(n)\mathbf{x}(n)]$ is the cross-correlation vector between the desired and the input signals, and $\mathbf{R} = E[\mathbf{x}(n)\mathbf{x}^T(n)]$ is the correlation matrix of the input signal. As can be noted, the objective function $F(e(n))$ is a quadratic function of the tap-weight coefficients which allows for a straightforward solution for w, when vector **p** and matrix **R** are known. Note that **R** corresponds to the Hessian matrix of the objective function.

The gradient vector of the MSE function (2.4) related to the filter coefficients is given by

$$\begin{aligned} g_{\mathbf{w}} &= \frac{\partial \xi}{\partial \mathbf{w}} = [\frac{\partial \xi}{\partial w_0} \frac{\partial \xi}{\partial w_1} \cdots \frac{\partial \xi}{\partial w_N}]^T \\ &= -2\mathbf{p} + 2\mathbf{R}\mathbf{w} \end{aligned} \tag{2.5}$$

By equating the gradient vector to zero and assuming **R** is non-singular, the optimal tap-weight vector that minimizes the objective function can be obtained as:

$$\mathbf{w}_0 = \mathbf{R}^{-1}\mathbf{p} \tag{2.6}$$

This solution is called the Wiener solution, which requires the exact knowledge of **R** and **p**. In practice, however, **R** and **p** are not available. Therefore, in most of adaptive algorithms **R** and **p** are estimated through time-domain average and the resulting solution is considered as an approximation of the Wiener solution.

2.3 Steepest-Descent Algorithm

The method of steepest-descent (SD) can be considered an efficient gradient-type algorithm that updates the weight vector at each iteration step. In order to get a practical feeling of a problem that is being solved using the steepest-descent algorithm, we assume that the optimal coefficient vector is given by the Wiener solution $\mathbf{w}_0$, and that the reference signal is not corrupted by measurement noise [12].

The SD algorithm updates the coefficients in the following general manner [12]

$$\mathbf{w}(n+1) = \mathbf{w}(n) - \frac{1}{2}\mu g_{\mathrm{w}}(n) \tag{2.7}$$

It is worth-noting that several alternative gradient-based algorithms are available to replace $g_{\mathrm{w}}(n)$ by $\hat{g}_{\mathrm{w}}(n)$, which differ in the way the gradient vector is estimated. Substituting equation (2.5) into equation (2.7), we get

$$\mathbf{w}(n+1) = \mathbf{w}(n) - \mu\mathbf{R}\mathbf{w}(n) + \mu\mathbf{p} \tag{2.8}$$

To look into the convergence behaviour of the SD algorithm in stationary environment, it is necessary to perform an analysis of the influence of the convergence factor μ on the adaptive algorithm.

The derivation of the filter coefficients from the Wiener solution is given by

$$\Delta\mathbf{w}(n) = \mathbf{w}(n) - \mathbf{w}_0 \tag{2.9}$$

The SD algorithm can then be represented in an alternative way, that is

$$\begin{aligned}\Delta\mathbf{w}(n+1) &= \Delta\mathbf{w}(n) - \mu(\mathbf{R}\mathbf{w}(n) + \mathbf{R}\mathbf{w}_0) \\ &= \Delta\mathbf{w}(n) - \mu\mathbf{R}\Delta\mathbf{w}(n) \\ &= (\mathbf{I} - \mu\mathbf{R})\Delta\mathbf{w}(n)\end{aligned} \tag{2.10}$$

where the relation $\mathbf{p}=\mathbf{R}\mathbf{w}_0$ has been employed in obtaining equation (2.10). It can easily be shown that

$$\Delta\mathbf{w}(n+1) = (\mathbf{I} - \mu\mathbf{R})^{n+1}\Delta\mathbf{w}(0) \tag{2.11}$$

Pre-multiplying equation (2.11) by Q^T, where Q is the unitary matrix that diagonalizes **R**, we have

$$\begin{aligned}\mathbf{Q}^T\Delta\mathbf{w}(n+1) &= (\mathbf{I} - \mu\mathbf{Q}^T\mathbf{R}\mathbf{Q})\mathbf{Q}^T\Delta\mathbf{w}(n) \\ &= \mathbf{v}(n+1) \\ &= (\mathbf{I} - \mu\Lambda)\mathbf{v}(n) \\ &= \begin{bmatrix} 1-\mu\lambda_0 & 0 & \cdots & 0 \\ 0 & 1-\mu\lambda_1 & & 0 \\ \vdots & 0 & \ddots & \vdots \\ 0 & 0 & & 1-\mu\lambda_N \end{bmatrix}\mathbf{v}(n)\end{aligned} \tag{2.12}$$

where

$$\mathbf{v}(n+1) = \mathbf{Q}^T\Delta\mathbf{w}(n+1) \tag{2.13}$$

is the rotated coefficient-vector error. Using mathematical induction, equation (2.12) can be rewritten as

$$\mathbf{v}(n+1) = (\mathbf{I} - \mu\Lambda)^{n+1}\mathbf{v}(0)$$

$$= \begin{bmatrix} (1-\mu\lambda_0)^{n+1} & 0 & \cdots & 0 \\ 0 & (1-\mu\lambda_1)^{n+1} & & 0 \\ \vdots & 0 & \ddots & \vdots \\ 0 & 0 & & (1-\mu\lambda_N)^{n+1} \end{bmatrix} \mathbf{v}(0) \qquad (2.14)$$

It is clear form (2.14) that in order to guarantee the convergence of the update algorithm, each element $1-\mu\lambda_i$ must have an absolute value less than one, which requires the convergence factor μ to satisfy

$$0 < \mu < \frac{2}{\lambda_{\max}} \qquad (2.15)$$

where $\lambda_{\max}$ is the largest eigenvalue of **R**. In this case, all the elements of the diagonal matrix in equation (2.14) tend to zero as $n \to \infty$, leading **v**(n+1) to **0** for large n. The above range of μ guarantees that the coefficient vector approaches the optimum solution $\mathbf{w}_0$. It should be mentioned that if matrix **R** has a large eigenvalue spread which is the ratio of the largest over the smallest eigenvalue, the convergence speed will be primarily dependent on the value of the smallest eigenvalue of **R**. Note that the slowest decaying element is given by $(1-\mu\lambda_{\min})^{n+1}$.

There are certain limitations in SD algorithm that **R** and **p** are usually unknown. Therefore, these values have to be estimated from the available data. The least-mean square (LMS) algorithm as one of the most frequently used adaptive algorithms will be introduced.

2.4 Least Mean Square (LMS) Algorithm

The LMS algorithm has been the most widely used algorithm in adaptive filtering for several reasons. These include its low computational complexity, guarantee of convergence in stationary environments, unbiased mean to the Wiener solution and stable behavior in finite-precision arithmetic implementation. As such, it was used in the AEC applications [11], [13].

In the LMS algorithm, it is assumed that $d(n)$ and $x(n)$ are jointly wide-sense stationary (WSS), and if good estimates of matrix $\mathbf{R}$, denoted by $\hat{\mathbf{R}}(n)$, and of vector $\mathbf{p}$, denoted by $\hat{\mathbf{p}}(n)$, are available, according to equation (2.8), a steepest-descent-based algorithm can be used to search the Wiener solution as follows:

$$\begin{aligned}\mathbf{w}(n+1) &= \mathbf{w}(n) - \frac{1}{2}\mu\hat{g}_{\mathrm{w}}(n) \\ &= \mathbf{w}(n) - \mu\hat{\mathbf{R}}\mathbf{w}(n) + \mu\hat{\mathbf{p}} \end{aligned} \tag{2.16}$$

for n=0,1,2,..., where $\mathbf{w}(n) = [w_0(n), w_1(n), \cdots, w_{N-1}(n)]^T$, $\hat{g}_{\mathrm{w}}(n)$ represents an estimate of the gradient vector of the objective function with respect to the filter coefficients.

One possible solution is to estimate the gradient vector by employing instantaneous estimates for $\mathbf{R}$ and $\mathbf{p}$ as follows

$$\hat{\mathbf{R}}(n) = \mathbf{x}(n)\mathbf{x}^T(n) \tag{2.17}$$

$$\hat{\mathbf{p}}(n) = d(n)\mathbf{x}(n) \tag{2.18}$$

where $\mathbf{x}(n) = [x(n), x(n-1), \cdots, x(n-N+1)]^T$. The resulting gradient estimate is represented by

$$\hat{g}_w(n) = -2d(n)\mathbf{x}(n) + 2\mathbf{x}(n)\mathbf{x}^T(n)\mathbf{w}(n)$$

$$= -2\mathbf{x}(n)(d(n) + \mathbf{x}^T(n)\mathbf{w}(n))$$

$$= -2e(n)\mathbf{x}(n) \tag{2.19}$$

Substituting equation (2.19) into (2.16), the LMS algorithm can be summarized as [12]

Initialization

$$\mathbf{x}(n) = \mathbf{w}(n) = [0 \quad 0 \quad \cdots \quad 0]^T$$

Do for $n \geq 0$

$$e(n) = d(n) - \mathbf{x}^T(n)\mathbf{w}(n) \tag{2.20}$$

$$\mathbf{w}(n+1) = \mathbf{w}(n) - \mu e(n)\mathbf{x}(n) \tag{2.21}$$

In order to guarantee convergence of the coefficient in the mean, the convergence factor of the LMS algorithm μ should be chosen in the range of

$$0 < \mu < \frac{2}{tr[\mathbf{R}]} \tag{2.22}$$

Due to the slow convergence speed of the LMS algorithm, the normalized LMS (NLMS) algorithm as one of the major algorithms for increasing the convergence speed in linear adaptive filters was derived.

2.5 Normalized Least Mean Square (NLMS) Algorithm

If one wishes to increase the convergence speed of the LMS algorithm without using other special estimates of the input signal correlation matrix, a variable convergence factor or step size is a natural solution. The normalized LMS algorithm (NLMS) usually converges faster than the LMS algorithm, since it utilizes a variable convergence step size to minimize the instantaneous output error [12].

The NLMS filter is manifestation of the principle of the minimal disturbance. From one iteration to the next, the weight vector of the adaptive filter should be changed in a minimal manner, subject to a constraint imposed on the updated filter's output. To cast this principle in mathematical terms, let **w**(n) denote the old weight vector of the filter at iteration n and **w**(n+1) denote its updated weight vector at iteration n+1. We may then formulate the criterion for designing the NLMS algorithm as that of constrained optimization. Given tap-input vector $\mathbf{x}(n)=[x(n),x(n-1),\cdots,x(n-N+1)]^T$, and desired response $d(n)$, determine the updated weight vector **w**(n+1) so as to minimize the squared Euclidean norm of the change [14],

$$\delta\mathbf{w}(n+1)=\mathbf{w}(n+1)-\mathbf{w}(n) \tag{2.23}$$

Subject to the constraint

$$\mathbf{w}^T(n+1)\mathbf{x}(n)=d(n) \tag{2.24}$$

To solve this constrained optimization problem, we use the method of lagrange multipliers. According to this method, the cost function for the problem at hand consists of two terms,

$$\text{J(n)}=\|\delta\mathbf{w}(n+1)\|^2+\lambda(d(n)-\mathbf{w}^T(n+1)\mathbf{x}(n)) \tag{2.25}$$

where λ is the lagrange multiplier.

The cost function J(n) is a quadratic function in $\mathbf{w}(n+1)$, as shown by expanding equation (2.25):

$$\text{J(n)}=(\mathbf{w}(n+1)-\mathbf{w}(n))^T(\mathbf{w}(n+1)-\mathbf{w}(n))+\lambda(d(n)-\mathbf{w}^T(n+1)\mathbf{x}(n)) \tag{2.26}$$

To find the optimum value of the updated weight vector that minimizes the cost function J(n), it is proposed as follows:

Differentiate the cost function J(n) with respect to $\mathbf{w}(n+1)$

$$\frac{\partial J(n)}{\partial \mathbf{w}(n+1)} = 2(\mathbf{w}(n+1) - \mathbf{w}(n)) - \lambda \mathbf{x}(n) \tag{2.27}$$

Setting the result in equation (2.27) equal to zero and solving for the optimal value $\mathbf{w}(n+1)$, we obtain

$$\mathbf{w}(n+1) = \mathbf{w}(n) + \frac{1}{2}\lambda \mathbf{x}(n) \tag{2.28}$$

Solve for the unknown multiplier λ by substituting equation (2.28) into the constraint equation (2.24), we first obtain

$$\begin{aligned} d(n) &= \mathbf{w}^T(n+1)\mathbf{x}(n) \\ &= (\mathbf{w}(n) + \frac{1}{2}\lambda \mathbf{x}(n))^T \mathbf{x}(n) \\ &= \mathbf{w}^T(n)\mathbf{x}(n) + \frac{1}{2}\lambda \|\mathbf{x}(n)\|^2 \end{aligned} \tag{2.29}$$

Then, solving for λ, we obtain

$$\lambda = \frac{2e(n)}{\|\mathbf{x}(n)\|^2} \tag{2.30}$$

where $e(n) = d(n) - \mathbf{w}^T(n)\mathbf{x}(n)$. Combining the results obtained to formulate the optimal value of the incremental change $\delta \mathbf{w}(n+1)$. Substituting equations (2.30) into (2.28), we have

$$\begin{aligned} \delta \mathbf{w}(n+1) &= \mathbf{w}(n+1) - \mathbf{w}(n) \\ &= \frac{1}{\|\mathbf{x}(n)\|^2} e(n)\mathbf{x}(n) \end{aligned} \tag{2.31}$$

In order to exercise control over the change in the tap-weight vector from one iteration to the next without changing the direction of the vector, we introduce a positive real scaling factor denoted by μ_{nlms}. We redefine equation (2.31) simply as

$$\delta\mathbf{w}(n+1) = \mathbf{w}(n+1) - \mathbf{w}(n)$$

$$= \frac{\mu_{nlms}}{\|\mathbf{x}(n)\|^2} e(n)\mathbf{x}(n) \tag{2.32}$$

Equivalently, we write

$$\mathbf{w}(n+1) = \mathbf{w}(n) + \frac{\mu_{nlms}}{\|\mathbf{x}(n)\|^2} e(n)\mathbf{x}(n) \tag{2.33}$$

By comparing the updating formula of the standard LMS algorithm with that of the NLMS algorithm, the desired upper bound result follows [12]:

$$0 < \mu = \frac{\mu_{nlms}}{tr[\mathbf{R}]} < \frac{2}{tr[\mathbf{R}]} \tag{2.34}$$

$$0 < \mu_{nlms} < 2 \tag{2.35}$$

Then, the NLMS algorithm is described as [12]

Initialization

$$\mathbf{x}(0) = \mathbf{w}(0) = [0 \quad 0 \quad \cdots \quad 0]^T$$

Choose $0 < \mu_{nlms} < 2$

γ =small constant

Do for $n \geq 0$

$$e(n) = d(n) - \mathbf{x}^T(n)\mathbf{w}(n) \tag{2.36}$$

$$\mathbf{w}(n+1) = \mathbf{w}(n) + \frac{\mu_{nlms}}{\gamma + \mathbf{x}^T(n)\mathbf{x}(n)} e(n)\mathbf{x}(n) \tag{2.37}$$

Due to the relatively fast convergence speed and low computational complexity, the NLMS algorithm has been applied into AEC [15], [16]. But this algorithm is still affected a lot by the eigenvalue spread of the input signal correlation matrix.

2.6 Recursive Least Square (RLS) Algorithm

The recursive least square (RLS) algorithms are known to pursue fast convergence even when the eigenvalue spread of the input signal correlation matrix is large. These algorithms have excellent performance when working in time-varying environments. Due to these merits, they have been used in AEC [17], [18]. But all these advantages come with the cost of an increased computational complexity and some stability problems, which are not as critical as in LMS-based algorithms [19]. The RLS algorithm will be introduced below.

The input signal information vector at a given instant n is given by

$$\mathbf{x}(n) = [x(n), x(n-1), \cdots, x(n-N+1)]^T \tag{2.38}$$

where N is the memory length of the FIR filter, the coefficients, $w_i(n)$ for i=0,1,...,N-1, are adaptable aiming at the minimization of a given objective function. In the case of least squares algorithms, the objective function is deterministic and is given by

$$\begin{aligned} \xi^d(n) &= \sum_{i=0}^{n} \lambda^{n-i} e^2(i) \\ &= \sum_{i=0}^{n} \lambda^{n-i} [d(i) - \mathbf{x}^T(i)\mathbf{w}(n)]^2 \end{aligned} \tag{2.39}$$

where $\mathbf{w}(n) = [w_0(n), w_1(n), \cdots, w_{N-1}(n)]^T$ is the adaptive filter coefficient vector and $e(i)$ is the a posteriori output error at instant i. The parameter λ here is an exponential weighting factor that should be chosen in the range $0 << \lambda \leq 1$. This parameter is also called forgetting factor since the information of the distant past has an increasing negligible effect on the coefficient updating [12].

It should be noticed that in the development of the LMS and LMS-based algorithms we utilized the a priori error. In the RLS algorithm $e(n)$ is used to denote the a posteriori error whereas $e'(n)$ denotes the a priori error, because the a posteriori error will be our first choice in the development of the RLS-based algorithms.

As can be noted, each error consists of the difference between the desired signal and the filter output, using the most recent coefficient $\mathbf{w}(n)$, by differentiating $\xi^d(n)$ with respect to $\mathbf{w}(n)$, is follows that

$$\frac{\partial \xi^d(n)}{\partial \mathbf{w}(n)} = -2\sum_{i=0}^{n} \lambda^{n-i}\mathbf{x}(i)[d(i) - \mathbf{x}^T(i)\mathbf{w}(n)] \tag{2.40}$$

By equating the result of equation (2.40) to zero, it is possible to find the optimal vector $\mathbf{w}(n)$ that minimizes the least square error, through the following relation:

$$-2\sum_{i=0}^{n} \lambda^{n-i}\mathbf{x}(i)[d(i) - \mathbf{x}^T(i)\mathbf{w}(n)] = \begin{bmatrix} 0 \\ 0 \\ \vdots \\ 0 \end{bmatrix} \tag{2.41}$$

The resulting equation for the optimal coefficient vector $\mathbf{w}(n)$ is given by

$$\begin{aligned} \mathbf{w}(n) &= [\sum_{i=0}^{n} \lambda^{n-i}\mathbf{x}(i)\mathbf{x}^T(i)]^{-1} \sum_{i=0}^{n} \lambda^{n-i}\mathbf{x}(i)d(i) \\ &= \mathbf{R}_D^{-1}(n)\mathbf{P}_D(n) \\ &= \mathbf{S}_D(n)\mathbf{P}_D(n) \end{aligned} \tag{2.42}$$

where $\mathbf{R}_D(n)$ and $\mathbf{P}_D(n)$ are called the deterministic correlation matrix of the input signal and the deterministic cross-correlation vector between the input and desired signal, respectively. $\mathbf{S}_D(n)$ is the inverse of $\mathbf{R}_D(n)$. Rewrite equation (2.42) into

$$[\sum_{i=0}^{n} \lambda^{n-i}\mathbf{x}(i)\mathbf{x}^T(i)]\mathbf{w}(n) = \lambda[\sum_{i=0}^{n-1} \lambda^{n-i-1}\mathbf{x}(i)d(i)] + \mathbf{x}(n)d(n) \tag{2.43}$$

By considering that

$$\mathbf{R}_D(n-1)\mathbf{w}(n-1) = \mathbf{P}_D(n-1) \tag{2.44}$$

It follows that

$$\begin{aligned}[\sum_{i=0}^{n} \lambda^{n-i}\mathbf{x}(i)\mathbf{x}^T(i)]\mathbf{w}(n) &= \lambda\mathbf{P}_D(n-1) + \mathbf{x}(n)d(n) \\ &= \lambda\mathbf{R}_D(n-1)\mathbf{w}(n-1) + \mathbf{x}(n)d(n) \\ &= [\sum_{i=0}^{n} \lambda^{n-i}\mathbf{x}(i)\mathbf{x}^T(i) - \mathbf{x}(n)\mathbf{x}^T(n)]\mathbf{w}(n-1) + \mathbf{x}(n)d(n) \end{aligned} \tag{2.45}$$

Now define the a priori error as

$$e'(n) = d(n) - \mathbf{x}^T(n)\mathbf{w}(n-1) \tag{2.46}$$

Expressing $d(n)$ as a function of the a priori error and replacing the result into equation (2.45), it can be shown that

$$\mathbf{w}(n) = \mathbf{w}(n-1) + e'(n)\mathbf{S}_D(n)\mathbf{x}(n) \tag{2.47}$$

Then it is straightforward to generate a conventional RLS algorithm [12]:

Initialization

$$\mathbf{S}_D(-1) = \delta\mathbf{I}$$

where δ can be the inverse of an estimate of the input signal power

$$\mathbf{x}(-1) = \mathbf{w}(-1) = [0 \quad 0 \quad \cdots \quad 0]^T$$

Do for $n \geq 0$

$$e'(n) = d(n) - \mathbf{x}^T(n)\mathbf{w}(n-1) \tag{2.48}$$

$$\psi(n) = \mathbf{S}_D(n-1)\mathbf{x}(n) \tag{2.49}$$

$$S_D(n) = \frac{1}{\lambda}[S_D(n-1) - \frac{\psi(n)\psi^T(n)}{\lambda + \psi^T(n)\mathbf{x}(n)} \tag{2.50}$$

$$\mathbf{w}(n) = \mathbf{w}(n-1) + e'(n)\mathbf{S}_D(n)\mathbf{x}(n) \tag{2.51}$$

If necessary compute

$$y(n) = \mathbf{w}^T(n)\mathbf{x}(n) \tag{2.52}$$

$$e(n) = d(n) - y(n) \tag{2.53}$$

Chapter 3 Brief Review of Nonlinear AEC Approaches

3.1 General

The linear filtering techniques are known to be effective in a variety of applications in signal processing, telecommunications and control. In some applications, however, the use of linear filters is not sufficient. For example, in acoustic echo cancellation (AEC) where nonlinear distortions caused by the loudspeaker/amplifier occur, linear filters can only cancel or alleviate the linear echo, leaving the nonlinear distortions after the AEC, thus resulting in a degraded communication quality [20]. As presented in this chapter, we will introduce the nonlinear filtering techniques applicable to nonlinear case.

Recently, nonlinear filters have become a very important tool in solving the problem of AEC, where a nonlinear filter is employed to identify as close as possible the acoustic echo path that is found to be highly nonlinear [10]. The main source of nonlinearities in an echo path is caused by the loudspeaker and the power amplifier which are operated at the highest signal level of the transmission chain [4]. The fundamental principle of loudspeaker has never been changed since its invention. A loudspeaker has so complex structure to transform electric signal into mechanical signal and to radiate acoustic wave. In general, it produces both linear and nonlinear distortions. Nonlinear cone suspension

and uneven magnetic flux densities in the loudspeaker introduce nonlinear distortions at large cone displacement levels. In the meanwhile, at a high volume setting, saturation effects may occur in the power amplifier, producing gross nonlinearities in the system. These nonlinear distortions greatly impair the performance of acoustic echo cancellers [8]. In order to find more powerful tools to solve the nonlinear distortion problems in acoustic systems, researchers have made tremendous efforts to developing various types of nonlinear filtering techniques.

A general block diagram of a nonlinear system identification model is shown in Figure 3.1. When the nonlinearity is caused by the loudspeaker/amplifier [21] operated at its power limit, the memory of this nonlinear behaviour cannot be neglected due to the long time constants of the electro-mechanical system. To combat this kind of nonlinearity, adaptive systems with memory are required. In [22], adaptive Volterra filters (VFs) were proposed for nonlinear echo cancellation (AEC). The VF-based methods were further studied in [23], [24]. In these methods, modelling the nonlinear acoustic echo path with the VF is essential to the elimination of the nonlinear distortion [25], [26]. However, due to its high numerical complexity, the VF has to be truncated and simplified to keep the computational complexity modest before its use in practical systems. On the other hand, if the major cause of nonlinearity is due to a clipping amplifier [4], namely, the amplifier will amplify the signal only up to its maximum capacity, at which point the signal will be amplified no further, a low-complexity scheme by using a memoryless saturation curve to describe this nonlinearity can be used to achieve a remarkable performance. As there is a lack of unique theory to model and characterize an arbitrary nonlinear system, we here introduce the basic nonlinear echo cancellation techniques based on VFs and a saturation-

type transform, which will be used to develop new AEC methods in the following chapters.

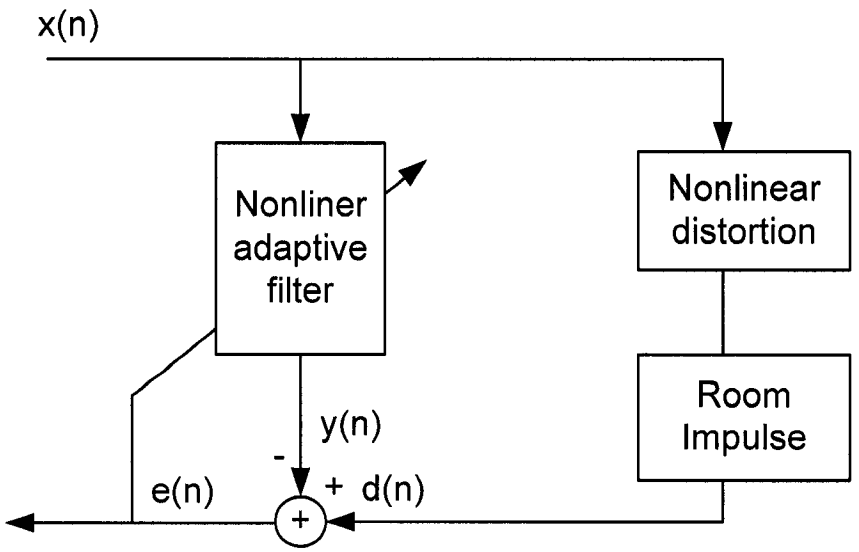

Figure 3.1 Nonlinear system identification model

3.2 Volterra Filter-Based AECs

The VF has been widely used as a nonlinear model in AEC [10], [20]. A VF is actually a truncated version of the Volterra series with finite order and memory. Given an input signal $x(n)$, the output of a nonlinear system using the *kth* order VF can be written as

$$y(n)=\sum_{i_1=0}^{N_1-1}h_1(i_1)x(n-i_1)+\sum_{i_1=0}^{N_2-1}\sum_{i_2=0}^{N_2-1}h_2(i_1,i_2)x(n-i_1)x(n-i_2)+\sum_{i_k=0}^{N_k-1}\cdots\sum_{i_k=0}^{N_k-1}h_k(i_1,\cdots,i_k)x(n-i_1)\cdots x(n-i_k) \tag{3.1}$$

where $h_1(i_1), h_2(i_1,i_2)\ldots\ h_k(i_1,\ldots i_k)$, for k=1,2..., are the coefficients of the VF model and in particular, the set $h_k(i_1,\ldots i_k)$ is also known as the *kth* order Volterra kernel of the

nonlinear filter [12]. In equation (3.1), N_k stands for the memory of the *kth* order kernel of the VF. Note that the Volterra kernels are usually assumed to be symmetric. For example, a 2nd order VF has a symmetric 2nd order kernel as given by $h_2(i_1,i_2)=h_2(i_2,i_1)$. Figure 3.2 shows an implementation diagram for a 2nd order VF with a memory length of 3 for each kernel. In which there are total 3 coefficients for the linear kernel, and a total of 6 coefficients for the

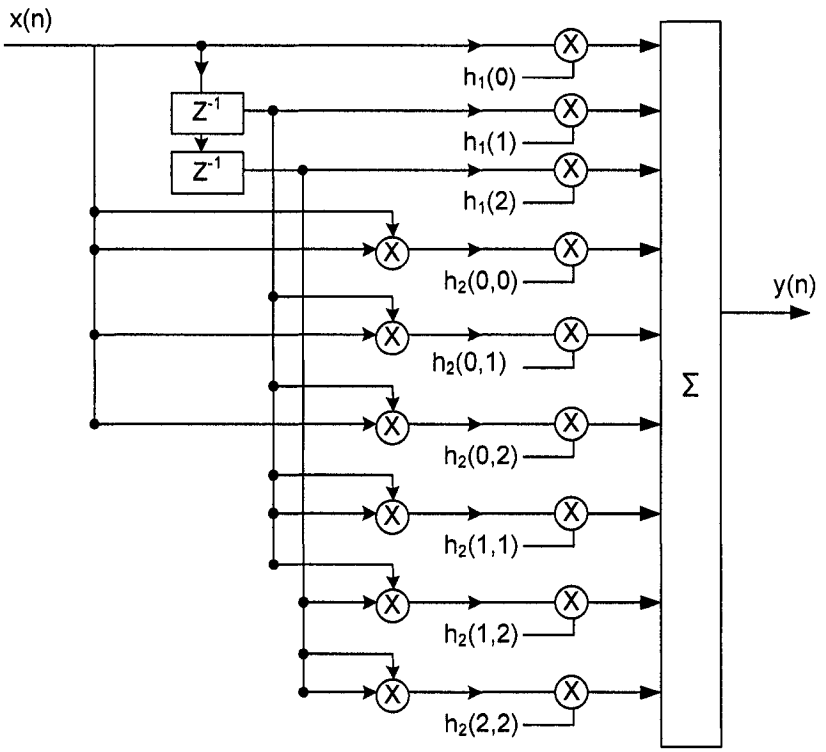

Figure 3.2 A 2nd order Volterra filter with two delay elements

2nd order kernel due to the symmetry. It is also clear that the output of the VF is a linear combination of the delayed versions of the input signal and their products yielding higher-order nonlinear terms. Accordingly, the output of a general VF can be expressed using vectors as [27]

$$y(n) = \mathbf{h}^T(n)\mathbf{x}(n) \tag{3.2}$$

where **h**(n) is comprised of all the VF parameters, namely,

$$\mathbf{h}(n)=[h_1(0;n), h_1(1;n)\cdots h_1(N_1-1;n), h_2(0,0;n), h_2(0,1;n),\cdots, h_2(N_2-1, N_2-1;n),\cdots]^T \tag{3.3}$$

and, the input vector $\mathbf{x}(n)$ of the VF is given by,

$$\mathbf{x}(n) = [x(n), x(n-1)\cdots x(n-N_1+1), x^2(n), x(n)x(n-1),\cdots, x^2(n-N_2+1),\cdots]^T \tag{3.4}$$

Note that equation (3.2) can be rewritten using the kernels of the VF as,

$$\begin{aligned} y(n) &= \mathbf{h}^T(n)\mathbf{x}(n) \\ &= [\mathbf{h}_1^T(n), \mathbf{h}_2^T(n),\cdots \mathbf{h}_k^T(n),\cdots] \begin{bmatrix} \mathbf{x}_1(n) \\ \mathbf{x}_2(n) \\ \vdots \\ \mathbf{x}_k(n) \\ \vdots \end{bmatrix} \end{aligned} \tag{3.5}$$

where $\mathbf{h}_k(n)$ is the coefficient vector of the *kth* order kernel and $\mathbf{x}_k(n)$ presents the input sub-vector corresponding to the *kth* order kernel.

Note that the input vector needs to be updated for every new sample of the input signal in order to calculate $y(n)$. It can be seen that, except the way the input vector is constructed, the VF behaves similar to a linear filter. Therefore, the VF is often treated as a linear filter and many linear adaptive algorithms can be applied directly to the VF, such as [27], [28], [29].

Broadly speaking, there are two kinds of VF-based structures. One is to use a conventional VF to model the whole nonlinear echo path including the effect of the loudspeaker and the room impulse response. In this structure, a VF with a large memory length and in turn a large number of coefficients is often required. Since the number of coefficients grows exponentially with the increase of the memory length, a direct use of

VF with large memory size incurs a slow convergence rate as well as a high computational complexity. The other is to model the echo path with a nonlinear cascade filter structure as studied in [30]. This structure consists of a VF for the modeling of the loudspeaker and a linear transversal filter to identify the room impulse response. The advantage of the cascade structure is its relatively low computational burden since the memory sizes for both the VF and the linear filters are short [30]. However, since the output of the entire cascade structure is a bilinear function of the filter coefficients, convergence toward the optimal solution cannot be guaranteed. Indeed, the non-quadratic form of the MSE in this scheme produces some local minima, leading to a convergence toward incorrect parameters if the initial values are not chosen properly. Both of the above AEC schemes are presented below, based on which a new approach using 2^{nd} order VF will be developed in Chapter 4.

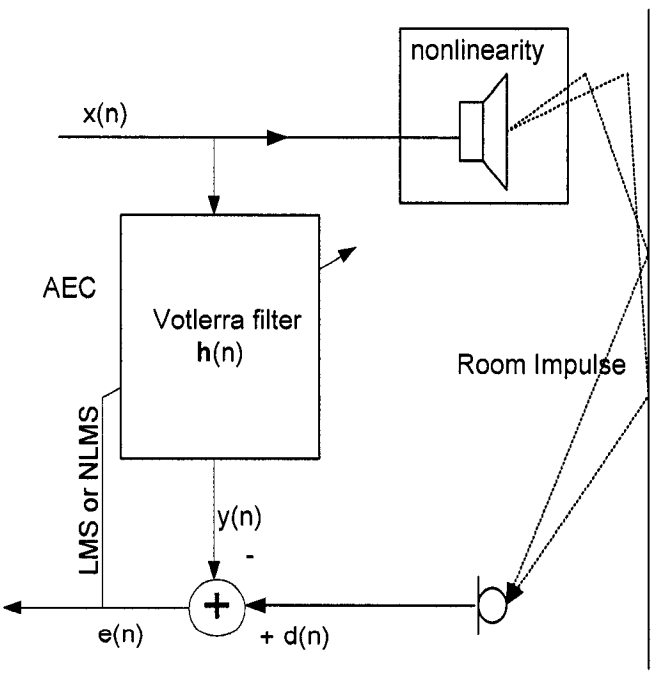

Figure 3.3 A Nonlinear AEC with adaptive Volterra filter

Figure 3.3 shows the block diagram of an adaptive VF. Since the adaptive VF is a direct extension of a linear adaptive filter, many linear filtering algorithms can be applied to the VF. For example, both LMS and normalized LMS (NLMS) algorithms have relatively low complexity and fast convergence speed, and therefore, find wide applications in AEC. The two basic algorithms for their application to VF are given as follows.

The LMS adaptive VF was proposed in [28], which states

Initialization

Specify the initial values $\mathbf{x}(0)$ and $\mathbf{h}(0)$

Do for $n \geq 0$

$$e(n) = d(n) - \mathbf{x}^T(n)\mathbf{h}(n) \tag{3.6}$$

$$\mathbf{h}(n+1) = \mathbf{h}(n) + \mu e(n)\mathbf{x}(n) \tag{3.7}$$

$$0 < \mu < \frac{2}{\lambda_{\max}} \tag{3.8}$$

---

where μ is the step size of iteration and $\lambda_{\max}$ is the maximum eigenvalue of the correlation matrix of the input vector $\mathbf{x}(n)$ of the VF. Alternatively, another LMS algorithm can be described via the Volterra kernels as

---

Initialization

Specify the initial values $\mathbf{x}_k(0)$ and $\mathbf{h}_k(0)$

Do for $n \geq 0$

$$e(n) = d(n) - \mathbf{x}_1^T(n)\mathbf{h}_1(n) - \mathbf{x}_2^T(n)\mathbf{h}_2(n)\cdots \tag{3.9}$$

for k=1,2...

$$\mathbf{h}_k(n+1) = \mathbf{h}_k(n) + \mu_k e(n)\mathbf{x}_k(n) \tag{3.10}$$

$$0 < \mu_k < \frac{2}{\lambda_{k,\max}} \tag{3.11}$$

---

where μ_k represents the step size for the *kth* kernel and $\lambda_{k,\max}$ is the largest eigenvalue of the input correlation matrix corresponding to the *kth* kernel. Like a general LMS algorithm, the convergence speed of the LMS adaptive VF depends on the eigenvalue spread, $\lambda_{\max} / \lambda_{\min}$, where $\lambda_{\min}$ is the smallest eigenvalue of the correlation matrix of $\mathbf{x}(n)$. It is obvious that the larger the eigenvalue spread, the slower the convergence speed is. This is particularly troublesome for nonlinear filters, since the eigenvalue spreads of nonlinear filters are in general very large. For accelerating the convergence of the adaptive VF, the NLMS algorithm is usually applied.

The NLMS algorithm for the VF can be stated as [27]

Initialization

Specify the initial values $\mathbf{x}(0)$ and $\mathbf{h}(0)$

Do for $n \geq 0$

$$e(n) = d(n) - \mathbf{x}^T(n)\mathbf{h}(n) \tag{3.12}$$

$$\mathbf{h}(n+1) = \mathbf{h}(n) + \frac{\mu_{nlms}}{\|\mathbf{x}(n)\|^2} e(n)\mathbf{x}(n) \tag{3.13}$$

$$0 < \mu_{nlms} < 2 \tag{3.14}$$

Similarly, the kernel version of the NLMS for the VF can also be described as

---

Initialization

Specify the initial values $\mathbf{x}_k(0)$ and $\mathbf{h}_k(0)$

Do for $n \geq 0$

$$e(n) = d(n) - \mathbf{x}_1^T(n)\mathbf{h}_1(n) - \mathbf{x}_2^T(n)\mathbf{h}_2(n) - \cdots \tag{3.15}$$

for k=1,2...

$$\mathbf{h}_k(n+1) = \mathbf{h}_k(n) + \frac{\mu_{nlms}}{\|\mathbf{x}_1(n)\|^2 + \cdots + \|\mathbf{x}_k(n)\|^2} e(n)\mathbf{x}_k(n) \tag{3.16}$$

$$0 < \mu_{nlms} < 2 \tag{3.17}$$

The NLMS adaptive VF also encounters some problems. Taking a 2nd order VF as an example, if $\|\mathbf{x}_1\|^2 >> \|\mathbf{x}_2\|^2$, the coefficients of the 2nd order kernel will be updated in a very small step according to constraint (3.17), which severely slows down the 2nd order kernel convergence [4].

The above VF structure treats the loudspeaker and the room impulse as an overall nonlinear system. In practice, however, the nonlinear loudspeaker and the linear room impulse response are in cascade connection nature, whereas the VF is considered as a parallel connection of a linear kernel and higher-order nonlinear kernels. Therefore, a general VF model cannot effectively identify the overall effect of the nonlinear loudspeaker and the linear room impulse response, because it is difficult to accurately choose the valid coefficients. Considering a VF can also accurately model the nonlinearity caused by the loudspeaker, another echo cancellation structure that is based on the cascade connection of a VF and a linear filter was proposed in [30] to identify the loudspeaker parameters and the room impulse response separately. Figure 3.4 shows the diagram of

such a cascaded-form nonlinear canceller, where the loudspeaker parameters are identified by a VF and the output signal of the VF feeds a transversal filter which is to identify the room impulse response.

The NLMS algorithm for the cascade structure can be summarized as [30]

$$\mathbf{x}(n) = [\mathbf{x}_1^T(n), \mathbf{x}_2^T(n), \cdots]^T$$

$$\mathbf{h}(n) = [\mathbf{h}_1^T(n), \mathbf{h}_2^T(n), \cdots]^T$$

$$\mathbf{w}(n) = [w_0(n), w_1(n), \cdots, w_{L-1}(n)]^T$$

$$\mathbf{U}_k(n) = [\mathbf{x}_k(n), \mathbf{x}_k(n-1), \cdots, \mathbf{x}_k(n-L+1)]^T \tag{3.18}$$

$$\mathbf{U}^T(n) = [\mathbf{x}(n), \mathbf{x}(n-1), \cdots, \mathbf{x}(n-L+1)] = [\mathbf{U}_1(n), \mathbf{U}_2, \cdots]^T \tag{3.19}$$

Initialization

Specify the initial values $\mathbf{h}(0)$ and $\mathbf{w}(0)$

Do for $n \geq 0$

$$\mathbf{x}_v(n) = \mathbf{U}(n)\mathbf{h}(n) \tag{3.20}$$

$$e(n) = d(n) - \mathbf{x}_v^T(n)\mathbf{w}(n) \tag{3.21}$$

$$\mathbf{w}(n+1) = \mathbf{w}(n) + \frac{\mu_w}{\|\mathbf{x}_v(n)\|^2} e(n)\mathbf{x}_v(n) \tag{3.22}$$

for k=1,2...

$$\mathbf{h}_k(n+1) = \mathbf{h}_k(n) + \frac{\mu_k}{\|\mathbf{U}_k^T(n)\mathbf{w}(n)\|^2} e(n)\mathbf{U}_k^T(n)\mathbf{w}(n) \tag{3.23}$$

$$0 < \mu_w, \mu_k < 2 \tag{3.24}$$

---

where $\mathbf{h}_k(n)$ is the *kth* order Volterra kernel, and L denote the memory length of the linear filter. The details of the NLMS-based nonlinear AEC can be found in [30].

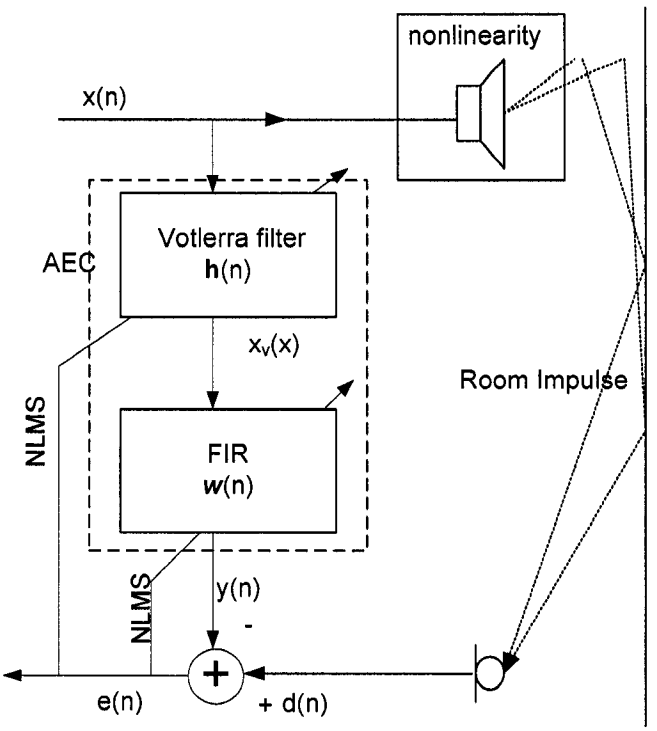

Figure 3.4 A cascade-form adaptive nonlinear AEC using VF

The two AEC structure along with their NLMS algorithms will be revisited in Chapter 4 in order to develop a simplified VF echo canceller.

3.3 Nonlinear Transform-Based AECs

The so-called memoryless nonlinearity a type of nonlinear distortion can be characterized by a saturation curve. This often occurs in power amplifiers, especially in mobile devices. In this situation, the nonlinear distortion in echo path can be modeled by a saturation-type nonlinear transform which is used to compensate the nonlinear distortion in conjunction with a liner FIR filter used to compensate the room impulse response. In [31], a general solution for this kind of distortion cancellation was introduced. Figure 3.5 shows the diagram of such a nonlinear transform-based acoustic echo canceller.

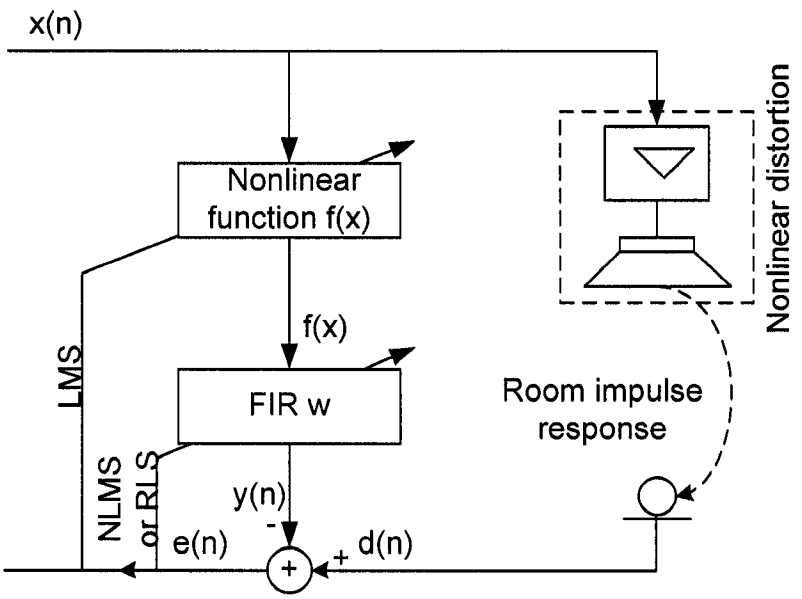

Figure 3.5 Block diagram of a typical nonlinear transform-based acoustic echo canceller

Several nonlinear transforms have already been proposed in literature for nonlinear AEC. For example, a hard-clipping nonlinear function as given by

$$f(a,x)=\begin{cases} -a & x \le -a \\ x & x < a \\ a & x \ge a \end{cases} \tag{3.25}$$

was adopted as a preprocessor in [31], prior to the linear adaptive filtering. The overall nonlinear AEC utilizing $f(a,x)$ along with a transversal filter was then updated via the NLMS algorithm, which is highlighted as follows.

Initialization

Specify the initial values $\mathbf{w}(0)$ and a_0

Do for $n \geq 0$

$$\mathbf{x}(n) = [x(n), x(n-1), \cdots, x(n-L+1)]^T \tag{3.26}$$

$$\mathbf{s}(n) = f(a_n, \mathbf{x}(n)) \tag{3.27}$$

$$\mathbf{s}(n) = [s(n), s(n-1), \cdots, s(n-L+1)]^T \tag{3.28}$$

$$e(n) = d(n) - \mathbf{w}^T(n) f(a_n, \mathbf{x}(n)) \tag{3.29}$$

$$a_{n+1} = a_n + \mu_a (f'(a_n, \mathbf{x}(n))^T \mathbf{w}(n) e(n) \tag{3.30}$$

$$\mathbf{w}(n+1) = \mathbf{w}(n) + \frac{\mu_w}{\|\mathbf{s}(n)\|^2} \mathbf{s}(n) e(n) \tag{3.31}$$

In the above algorithm, L denote the memory length of the FIR filter. μ_a and μ_w are the step sizes for the update of the parameters a and the coefficients vector of the FIR filter, respectively. Note that $f(a_n, \mathbf{x}(n))$ is a vector representing the distortion version of $\mathbf{x}(n)$ and $f'(a_n, \mathbf{x}(n))$ is the first derivative of $f(a_n, \mathbf{x}(n))$ with respect to a_n. This method is just suitable for the hard-clipping distortion situation.

Recently, a novel nonlinear AEC has been proposed in [32], where nonlinear transform based on the raised-cosine function is used to compensate the nonlinearity of the power amplifier. The nonlinearly transformed signal is then processed by a conventional linear adaptive filter. This nonlinear filter has been proved to perform well in AEC. In this nonlinear canceller, the nonlinear transform was derived from the raised-cosine function and can be eventually expressed as

$$f(x)=\begin{cases} -1, & x<-\dfrac{1+\beta}{2T} \\ Tx-\dfrac{1-\beta}{2}-\dfrac{\beta}{\pi}\cos[\dfrac{2Tx\pi+\pi}{2\beta}], & -\dfrac{1+\beta}{2T}\le x\le -\dfrac{1-\beta}{2T} \\ 2Tx, & -\dfrac{1-\beta}{2T}\le x\le \dfrac{1-\beta}{2T} \\ Tx+\dfrac{1-\beta}{2}+\dfrac{\beta}{\pi}\cos[\dfrac{2Tx\pi-\pi}{2\beta}], & \dfrac{1-\beta}{2T}\le x\le \dfrac{1+\beta}{2T} \\ 1, & x>\dfrac{1+\beta}{2T} \end{cases} \tag{3.32}$$

where T and β are the free parameters to determine the shape and the dynamic range of the nonlinear curve. The significant advantage of the transform given by equation (3.32) is its capability of fitting a wide range of saturation curves through a proper choice of the values of T and β. The algorithm is summarized below

---

Initialization

Specify the initial values, $\mathbf{w}(0), T_0$ and β_0

Do for $n \ge 0$

$$e(n) = d(n) - \mathbf{w}^T(n) f(\mathbf{x}(n)) \tag{3.33}$$

$$\beta_{n+1} = \beta_n + \mu_\beta e(n)\mathbf{w}^T(n)\frac{\partial f(\mathbf{x}(n))}{\partial \beta}\Big|_{\beta=\beta_n, T=T_n} \tag{3.34}$$

where $\dfrac{\partial f(\mathbf{x}(n))}{\partial \beta} =$

$$\begin{cases} 0, & |x|<\dfrac{1-\beta}{2T} \text{ or } |x|>\dfrac{1+\beta}{2T} \\ \dfrac{1}{2}-\dfrac{1}{\pi}\cos\left(\dfrac{2Tx\pi+\pi}{2\beta}\right)-\dfrac{2Tx+1}{2\beta}\sin\left(\dfrac{2Tx\pi+\pi}{2\beta}\right), & -\dfrac{1-\beta}{2T}\le x<\dfrac{1-\beta}{2T} \\ -\dfrac{1}{2}+\dfrac{1}{\pi}\cos\left(\dfrac{2Tx\pi-\pi}{2\beta}\right)+\dfrac{2Tx-1}{2\beta}\sin\left(\dfrac{2Tx\pi-\pi}{2\beta}\right), & \dfrac{1-\beta}{2T}<x\le\dfrac{1+\beta}{2T} \end{cases}$$

$$T_{n+1} = T_n + \mu_T e(n)\mathbf{w}^T(n)\frac{\partial f(\mathbf{x}(n))}{\partial T}\Big|_{T=T_n,\beta=\beta_n} \tag{3.35}$$

where $$\frac{\partial f(\mathbf{x}(n))}{\partial T} = \begin{cases} 2x, & |x| < \dfrac{1-\beta}{2T} \\ x + x\sin\left(\dfrac{2Tx\pi + \pi}{2\beta}\right), & -\dfrac{1-\beta}{2T} \le x < \dfrac{1-\beta}{2T} \\ x - x\sin\left(\dfrac{2Tx\pi - \pi}{2\beta}\right), & \dfrac{1-\beta}{2T} < x \le \dfrac{1+\beta}{2T} \\ 0, & |x| > \dfrac{1+\beta}{2T} \end{cases}$$

$$\mathbf{w}(n+1) = \mathbf{w}(n) + \frac{\mu}{\|f(\mathbf{x}(n))\|^2} f(\mathbf{x}(n))e(n) \tag{3.36}$$

---

where $\mathbf{w}(n)$ represents the coefficient vector of the transversal filter, and $\mathbf{x}(n)$ is the signal vector input to the nonlinear transformer. μ_β, μ_T and μ are the step sizes. Note that $f(\mathbf{x}(n))$ represents a vector that is the distorted version of $\mathbf{x}(n)$.

It has been shown in [32] that the update of parameters T and β can easily be implemented with the derived explicit update formulas. Moreover, the convergence of T and β does not depend on their initial values. However, due to the high complexity of the nonlinear transform which is piecewise defined, the convergence of T and β could not have been justified theoretically.

In summary, the nonlinear transform-based echo cancellation methods are very efficient in dealing with the saturation-type nonlinear distortions. Furthermore, they enjoy a very low computational complexity as compared to the VF-based nonlinear AECs. Motivated by the simplicity of the nonlinear transform method, a new nonlinear echo canceller that uses a sigmoid function in conjunction with a conventional FIR filter will be proposed in Chapter 5 for the cancellation of the saturation-type distortions.

Chapter 4 A New AEC Based on a Simplified 2nd Order VF

To model accurately the nonlinearity caused by the loudspeaker in acoustic systems, a nonlinear filter with memory is required [4]. As the Volterra filter (VF) can be regarded as the Taylor series with memory and can be used to model any nonlinear distortions, an adaptive VF is commonly employed to model a loudspeaker or a complete echo path in AEC. Since a conventional VF suffers from a large number of parameters and in turn a high computational complexity [33] in modeling a complete nonlinear echo path, many researchers have dedicated to the reduction of computational complexity of VF to better meet the need of practical nonlinear acoustic echo cancellation (AEC) [10].

It has been observed that the 2nd order kernel of a VF, when used to model the whole echo path, has its most significant coefficients laying on the diagonals near the main one. Based on this observation, some simplified 2nd order VFs have been proposed [10], [34], [35]. Their common idea is to discard some insignificant coefficients of the 2nd order kernel, leading to a significantly reduced filter length. As mentioned in Chapter 3, the NLMS algorithm is often used in the VF-based AECs. However, the input correlation matrix of a VF is usually ill-conditioned due to the involvement of the product terms in the formed input signal vector, making the NLMS less efficient even in the case of

Gaussian input. Moreover, the convergence rate of the 2nd order VF is very sensitive to the variance of the input signal.

In this chapter, an efficient scheme is proposed to reduce greatly the insignificant coefficients of the 2nd order Volterra kernel when a VF is used to model the complete echo path. A NLMS algorithm using a new update mechanism for the step size is also presented for kernel-separated 2nd order VF to reduce the effect of ill-conditioning of the correlation matrix.

Section 4.1 presents a simplified structure of the 2nd order VF with theoretical justification. Section 4.2 derives a new NLMS algorithm for kernel-separated VF in which a new update scheme for the step size is utilized. An eigenvalue spread analysis of the new algorithm is also undertaken. Section 4.3 gives simulation results to validate the proposed simplification strategy as well as the new NLMS algorithm.

4.1 A New Simplified Structure of 2nd Order VF

As stated in the previous chapter, the overall echo path counting the loudspeaker and the room impulse response can be better modeled by a cascade of a Volterra filter and an FIR filter, rather than a single VF. However, the cascade VF structure has the convergence problem i.e. the coefficients of the cascade structure tend to converge to local minima. Figure 4.1 shows a nonlinear AEC using cascade VF structure consisting of a 2nd order VF $\mathbf{g}(n)$ and a linear filter $\mathbf{w}(n)$, in which it is assumed that the NLMS is applied to update both the nonlinear and linear filters. In this section, we will show that the cascade VF structure is exactly equivalent to another 2nd order VF $\mathbf{h}(n)$ with reduced 2nd order kernel coefficients. Moreover, the memory length of the new filter $\mathbf{h}(n)$ can be determined by

that of **g**(n) as well as **w**(n). the new 2nd order VF **h**(n) is referred to as the simplified 2nd order VF.

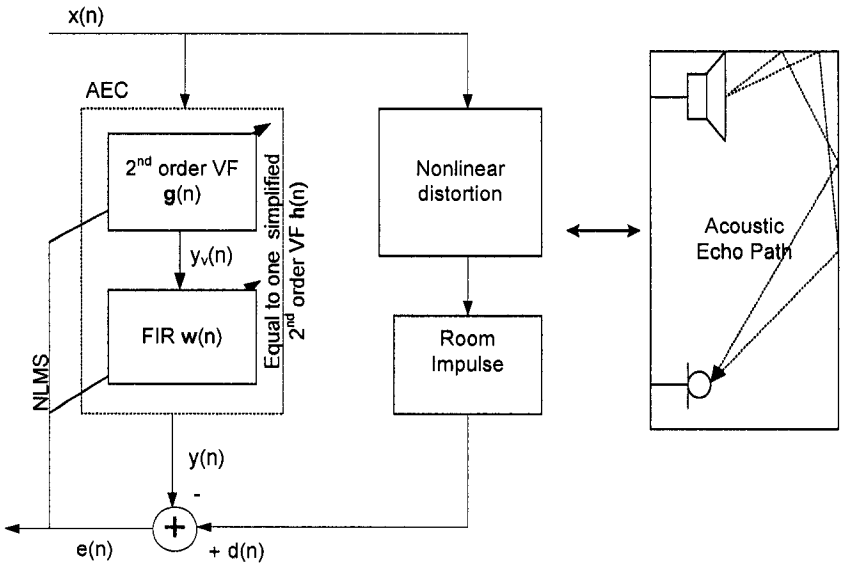

Figure 4.1 Nonlinear acoustic echo canceller using 2nd order VF

It has been shown in [25] that Volterra kernels are symmetric and thus, a 2nd order VF can be expressed as

$$y(n)=\sum_{i_1=0}^{N_1-1}h_1(i_1)x(n-i_1)+\sum_{i_2=0}^{N_2-1}\sum_{j_2=i_2}^{N_2-1}h_2(i_2,j_2)x(n-i_2)x(n-j_2) \qquad (4.1)$$

where N_1 and N_2 denote the memory lengths of the 1st and the 2nd order kernels, respectively. Considering that the coefficients with the most significant amplitude of the 2nd order kernel are located around the main diagonal, we propose a representation for the 2nd order kernel, namely

$$y(n)=\sum_{i_1=0}^{N_1-1}h_1(i_1)x(n-i_1)+\sum_{i_2=0}^{N_2-1}\sum_{j_2=i_2}^{N_2-1}h_2(j_2-i_2,j_2)x(n+i_2-j_2)x(n-j_2) \qquad (4.2)$$

where the 2nd order kernel coefficients are re-arranged in terms of the relative importance of the diagonal elements. Taking a 4-memory 2nd order Volterra kernel as an example, the

selection of the kernel coefficients starts from the most important main diagonal elements and extends then to the upper-triangle elements, as shown in the following equation,

$$\mathbf{H}_2=\begin{bmatrix} h_{00} & h_{01} & h_{02} & h_{03} \\ h_{10} & h_{11} & h_{12} & h_{13} \\ h_{20} & h_{21} & h_{22} & h_{23} \\ h_{30} & h_{31} & h_{32} & h_{33} \end{bmatrix} \tag{4.3}$$

where symbol $h_{i\,j}$ has been used to replace $h_2(i,j)$ for notational convenience. As will be seen later, with the new formulation one can easily drop insignificant coefficients by keeping several most important diagonals of $\mathbf{H}_2$.

In order to reveal the relationship between the cascade VF structure and the equivalent simplified VF, we first make following definitions,

$x(n)$: the input signal

$y_v(n)$: the output of the VF $\mathbf{g}$(n)

$y(n)$: the output of the entire cascade structure, namely, the estimate of the echo signal.

$d(n)$: the desired signal.

$\mathbf{g}(n)$: the vector of VF coefficients in which can be written as

$$\mathbf{g}(n)=\begin{bmatrix} \mathbf{g}_1(n) \\ \mathbf{g}_2(n) \end{bmatrix} \tag{4.4}$$

where

$$\mathbf{g}_1(n)=[g_0(n),g_1(n),g_2(n)\cdots,g_{N_1-1}(n)]^T \tag{4.5}$$

and

$$\mathbf{g}_2(n)=[g_{0\,0}(n),g_{1\,1}(n),g_{2\,2}(n),\cdots,g_{1\;N_2-1}(n),g_{0\;N_2-1}(n)]^T \tag{4.6}$$

$\mathbf{g}_1(n)$ and $\mathbf{g}_2(n)$ represent the 1st and 2nd order kernel vectors, respectively, in the cascade structure.

$\mathbf{u}(n)$: the input vector of the VF in the cascade structure, which can be expressed

$$\mathbf{u}(n)=\begin{bmatrix}\mathbf{u}_1(n)\\ \mathbf{u}_2(n)\end{bmatrix} \tag{4.7}$$

where

$$\mathbf{u}_1(n)=[x(n),x(n-1),x(n-2),\cdots,x(n-N_1+1)]^T \tag{4.8}$$

and

$$\mathbf{u}_2(n)=[x^2(n),x(n-1)x(n-1),x(n-2)x(n-2),\cdots,x(n-1)x(n-N_2+1),x(n)x(n-N_2+1)]^T \tag{4.9}$$

$\mathbf{u}_1(n)$ and $\mathbf{u}_2(n)$ represent the input vectors of the 1st and 2nd order Volterra kernels, respectively, in cascade structure.

$\mathbf{h}$(n): a vector of coefficients of the new VF,

$$\mathbf{h}(n)=\begin{bmatrix}\mathbf{h}_1(n)\\ \mathbf{h}_2(n)\end{bmatrix} \tag{4.10}$$

with $\mathbf{h}_1(n)$ and $\mathbf{h}_2(n)$ being the 1st and 2nd order kernel vectors, respectively, of the 2nd order VF to be determined.

$\mathbf{x}$(n): input vector of the new VF $\mathbf{h}$(n), as given by ,

$$\mathbf{x}(n)=\begin{bmatrix}\mathbf{x}_1(n)\\ \mathbf{x}_2(n)\end{bmatrix} \tag{4.11}$$

where $\mathbf{x}_1(n)$ and $\mathbf{x}_2(n)$ represent the input vectors of the 1st and 2nd order kernels of the VF, respectively.

We now derive the expression for the output $y(n)$ of the cascade structure in terms of **g**(n) and **w**(n) as well as that in terms of **h**(n) only. We will then show that the two expressions are equivalent provided that some of the 2nd order kernel coefficients in **h**(n) are set to zero.

Employing the above definition, $y_v(n)$ can be expressed in vector form as

$$y_v(n) = \mathbf{u}^T(n)\mathbf{g}(n) \tag{4.12}$$

Substituting equations (4.4) and (4.7) into equation (4.12), we obtain

$$\begin{aligned} y_v(n) &= \begin{bmatrix} \mathbf{u}_1(n) \\ \mathbf{u}_2(n) \end{bmatrix}^T \begin{bmatrix} \mathbf{g}_1(n) \\ \mathbf{g}_2(n) \end{bmatrix} \\ &= \mathbf{u}_1^T(n)\mathbf{g}_1(n) + \mathbf{u}_2^T(n)\mathbf{g}_2(n) \end{aligned} \tag{4.13}$$

Then, the output of the cascade structure can be expressed as

$$y(n) = \mathbf{w}^T(n)\mathbf{y}_v(n) \tag{4.14}$$

where $\mathbf{w}(n) = [w_0(n), w_1(n), \cdots, w_{N_r-1}(n)]$ denotes an N_r-tap FIR filter coefficients and $\mathbf{y}_v(n) = [\, y_v(n), y_v(n-1), \cdots, y_v(n-N_r+1)\,]$ is formed by $y_v(n)$ from equation (4.13), i.e.

$$y_v(n-i) = \begin{bmatrix} \mathbf{u}_1(n-i) \\ \mathbf{u}_2(n-i) \end{bmatrix}^T \begin{bmatrix} \mathbf{g}_1(n) \\ \mathbf{g}_2(n) \end{bmatrix} \tag{4.15}$$

Using equation (4.15), the vector $\mathbf{y}_v(n)$ can be expressed as

$$\begin{aligned} \mathbf{y}_v(n) &= \mathbf{U}^T(n)\mathbf{g}(n) \\ &= \begin{bmatrix} \mathbf{U}_1(n) \\ \mathbf{U}_2(n) \end{bmatrix}^T \begin{bmatrix} \mathbf{g}_1(n) \\ \mathbf{g}_2(n) \end{bmatrix} \end{aligned} \tag{4.16}$$

where $\mathbf{U}_1(n)$ is a N_1byN_r matrix formed by $\mathbf{u}_1(n)$, namely,

$$\mathbf{U}_1(n) = [\, \mathbf{u}_1(n), \mathbf{u}_1(n-1), \ldots, \mathbf{u}_1(n-N_r+1)\,] \tag{4.17}$$

and $\mathbf{U}_2(n)$ is a M_2byN_r matrix constituted by $\mathbf{u}_2(n)$ i.e.

$$\mathbf{U}_2(n)=[\mathbf{u}_2(n),\mathbf{u}_2(n-1),\ldots,\mathbf{u}_2(n-N_r+1)] \tag{4.18}$$

Note that the row dimension M_2 is determined by the following combination [142]

$$M_2=\binom{N_2+p-1}{p} \tag{4.19}$$

where, p=2 for the 2nd order VF.

Substituting equation (4.16) into equation (4.14), yields

$$y(n)=\mathbf{w}^T(n)\mathbf{U}_1^T(n)\mathbf{g}_1(n)+\mathbf{w}^T(n)\mathbf{U}_2^T(n)\mathbf{g}_2(n) \tag{4.20}$$

It is easy to verify that,

$\mathbf{w}^T(n)\mathbf{U}_1^T(n)\mathbf{g}_1(n)$

$$=[w_0(n),w_1(n),\cdots,w_{N_r-1}(n)]\begin{bmatrix} x(n) & x(n-1) & \cdots & x(n-N_1+1) \\ x(n-1) & x(n-2) & & x(n-N_1) \\ \vdots & & \ddots & \vdots \\ x(n-N_r+1) & \cdots & & x(n-N_1-N_r+2) \end{bmatrix}\begin{bmatrix} g_0(n) \\ g_1(n) \\ \vdots \\ g_{N_1-1}(n) \end{bmatrix} \tag{4.21}$$

$\mathbf{w}^T(n)\mathbf{U}_2^T(n)\mathbf{g}_2(n)$

$=[w_0(n),w_1(n),\cdots,w_{N_r-1}(n)]$

$$\begin{bmatrix} x^2(n) & x(n-1)x(n-1) & \cdots & x(n-1)x(n-N_2+1) & x(n)x(n-N_2+1) \\ x^2(n-1) & \vdots & x(n-1)x(n-2) & & x(n-1)x(n-N_2) \\ \vdots & & & \ddots & \vdots \\ x^2(n-N_r+1) & \cdots & x(n-N_r+1)x(n-N_r) & \cdots & x(n-N_r+1)x(n-N_2-N_r+2) \end{bmatrix}$$
$$\begin{bmatrix} g_{0\,0}(n) \\ g_{1\,1}(n) \\ \vdots \\ g_{0\,N_2-1}(n) \end{bmatrix} \tag{4.22}$$

On the other hand, the output of the new VF **h**(n) can be written as

$$y(n) = \mathbf{h}_1^T(n)\mathbf{x}_1(n) + \mathbf{h}_2^T(n)\mathbf{x}_2(n) \tag{4.23}$$

Considering the memory lengths of $\mathbf{g}_1(n)$ and $\mathbf{g}_2(n)$ as well as the lengths of **w**(n), the memory length of $\mathbf{h}_1(n)$ is set to N_1+N_r-1, and that for $\mathbf{h}_2(n)$ is N_2+N_r-1. In what follows, we show that equation (4.20) is equivalent to equation (4.23) provided that some of the coefficients of $\mathbf{h}_2(n)$ are set to zero.

It is obvious that equation (4.21) is equivalent to the first part $\mathbf{h}_1^T(n)\mathbf{x}_1(n)$ of the right hand side of equation (4.23) as long as $\mathbf{x}_1(n) = [x(n), x(n-1), \cdots, x(n-N_1-N_r+2)]^T$. As for the output of the 2nd order kernel $\mathbf{h}_2(n)$, $\mathbf{x}_2(n)$ can be written under the full memory length of N_2+N_r-1, as

$$\mathbf{x}_2(n) = [x^2(n), x(n-1)x(n-1), x(n-2)x(n-2), \cdots, x(n-1)x(n-N_2-N_r+2), x(n)x(n-N_2-N_r+2)]^T \tag{4.24}$$

It is seen from equation (4.22) that not all cross terms, such as $x(n)x(n-N_2)$, $x(n-N_r)x(n-N_2-N_r+2), \cdots, x(n)x(n-N_2-N_r+2)$ are not included, implying that a simplified version of $\mathbf{x}_2(n)$ should be applied in equation (4.23), which leads to a simplified structure of $\mathbf{h}_2(n)$. This result can be illustrated in the following matrix expression of the 2nd order kernel coefficients

$$\begin{bmatrix} h_{0,0} & h_{0,1} & \cdots & h_{0,N_2-1} & \cdots & h_{0,N_2+N_r-2} \\ h_{1,0} & h_{1,1} & & h_{1,N_2-1} & & h_{1,N_2+N_r-2} \\ \vdots & \vdots & & \vdots & & \vdots \\ h_{N_r-1,0} & h_{N_r-1,1} & & h_{N_r-1,N_2-1} & & h_{N_r-1,N_2+N_r-2} \\ \vdots & \vdots & & \vdots & & \vdots \\ h_{N_2+N_r-2,0} & h_{N_2+N_r-2,1} & \cdots & h_{N_2+N_r-2,N_2-1} & \cdots & h_{N_2+N_r-2,N_2+N_r-2} \end{bmatrix} \tag{4.25}$$

where only the coefficients marked within dashed line are required to form $\mathbf{h}_2(n)$, the 2nd

order kernel thus simplified along with the first order kernel is referred to as the simplified 2^{nd} order VF in this thesis.

4.2 A New NLMS Algorithm for Kernel-Separated 2^{nd} Order VF

4.2.1 Algorithm Derivation

In section 4.1, a simplified 2^{nd} order VF which is equivalent to a cascaded VF has been developed to model an acoustic echo path. As stated in Chapter 3, although the NLMS can be directly applied to a nonlinear VF, the convergence speed would be affected considerably by the existence of the nonlinear distortion because of the ill-conditioned correlation matrix of the input signal of the nonlinear VF. In this section, a new NLMS algorithm is proposed to update two kernels of the 2^{nd} order VF separately as described in Figure 4.2. as show later, this algorithm can reduce the effect of the ill-conditioning of the correlation matrix, thus speeding up the filter convergence rate.

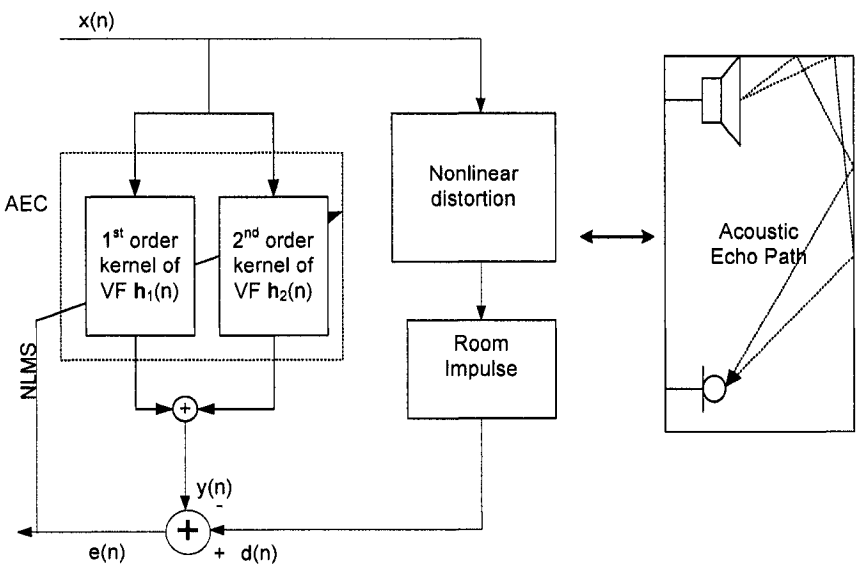

Figure 4.2 Kernel-separated structure of a 2^{nd} order VF

As denoted in Figure 4.2, the estimated error $e(n)$ can be expressed as

$$e(n) = d(n) - y(n) \tag{4.26}$$

Substituting equations (4.10) and (4.11) into equation (4.23), and using equation (4.26) we can obtain the mean-square-error (MSE) $J(n)$ as

$$J(n) = E[e^2(n)] = E[(d(n) - \mathbf{h}_1^T(n)\mathbf{x}_1(n) - \mathbf{h}_2^T(n)\mathbf{x}_2(n))^2] \tag{4.27}$$

Some researchers have considered to update the 1st and 2nd order kernels separately to overcome the slow convergence problem. In this methods, however, the choice of the step size μ follows a conventional NLMS scheme, which is not ideally suited for the two different kernels as whole, due to the interaction between them. Moreover, the range of μ is in conventional NLMS algorithm does not guarantee the convergence of the VF coefficients. To obtain a more efficient NLMS algorithm for kernel-separated 2nd order VF, we first establish two cost functions for the first and second order Volterra kernels, respectively as shown in Figure 4.2:

Minimize $\delta\mathbf{h}_1(n+1) = \mathbf{h}_1(n+1) - \mathbf{h}_1(n)$ (4.28a)

subject to the constraint $\mathbf{h}_1^T(n+1)\mathbf{x}_1(n) = d_1(n)$ (4.28b)

Minimize $\delta\mathbf{h}_2(n+1) = \mathbf{h}_2(n+1) - \mathbf{h}_2(n)$ (4.29a)

subject to the constraint $\mathbf{h}_2^T(n+1)\mathbf{x}_2(n) = d_2(n)$ (4.29b)

where $d_1(n)$ and $d_2(n)$ denote respectively, the desired signal of the first order kernel and that of the 2nd order one.

Following the method of lagrange multiplier [14], we have

$$J_i(n) = \|\delta\mathbf{h}_i(n+1)\|^2 + \lambda_i(d_i(n) - \mathbf{h}_i^T(n+1)\mathbf{x}(n)) \quad (i=1, 2) \tag{4.30}$$

By taking the derivative of $J_i(n)$ with respect to $\mathbf{h}_i(n+1)$, we can obtain

$$\frac{\partial J_1(n)}{\partial \mathbf{h}_1(n+1)} = 2(\mathbf{h}_1(n+1) - \mathbf{h}_1(n)) - \lambda_1 \mathbf{x}_1(n) \tag{4.31a}$$

$$\frac{\partial J_2(n)}{\partial \mathbf{h}_2(n+1)} = 2(\mathbf{h}_2(n+1) - \mathbf{h}_2(n)) - \lambda_2 \mathbf{x}_2(n) \tag{4.31b}$$

where λ_1 and λ_2 represent two different lagrange multipliers.

Letting (4.31a) and (4.31b) be zero, we obtain

$$\mathbf{h}_1(n+1) = \mathbf{h}_1(n) + \frac{1}{2}\lambda_1 \mathbf{x}_1(n) \tag{4.32a}$$

$$\mathbf{h}_2(n+1) = \mathbf{h}_2(n) + \frac{1}{2}\lambda_2 \mathbf{x}_2(n) \tag{4.32b}$$

Considering that only $d(n)$, instead of $d_1(n)$ and $d_2(n)$ individually, is available in practice, where

$$d_1(n) + d_2(n) = d(n) \tag{4.33}$$

we substitute equation (4.28b) and (4.29b) into equation (4.33) to produce

$$\mathbf{h}_1^T(n+1)\mathbf{x}_1(n) + \mathbf{h}_2^T(n+1)\mathbf{x}_2(n) = d(n) \tag{4.34}$$

Using equations (4.32a) and (4.32b) into (4.34), gives

$$d(n) - \mathbf{h}_1^T(n)\mathbf{x}_1(n) - \mathbf{h}_2^T(n)\mathbf{x}_2(n) = \frac{1}{2}\lambda_1 \mathbf{x}_1^T(n)\mathbf{x}_1(n) + \frac{1}{2}\lambda_2 \mathbf{x}_2^T(n)\mathbf{x}_2(n) \tag{4.35}$$

or

$$e(n) = \frac{1}{2}\lambda_1 \mathbf{x}_1^T(n)\mathbf{x}_1(n) + \frac{1}{2}\lambda_2 \mathbf{x}_2^T(n)\mathbf{x}_2(n) \tag{4.36}$$

Here, we can see λ_1 and λ_2 are jointly determine e(n). Following [14], let

$$\lambda_1 = \frac{2\mu_1 e(n)}{\mathbf{x}_1^T(n)\mathbf{x}_1(n)} \tag{4.37a}$$

$$\lambda_2 = \frac{2\mu_2 e(n)}{\mathbf{x}_2^T(n)\mathbf{x}_2(n)} \tag{4.37b}$$

where μ_1 and μ_2 are positive real scaling factors [14]. Substituting equations (4.37a) and (4.37b) into equation (4.36), one can verify that

$$\mu_1 + \mu_2 = 1 \tag{4.38}$$

On the other hand, using equations (4.37a) and (4.37b) into (4.32a) and (4.32b), respectively, the kernels of the 2nd order VF can be updated as follows

$$\mathbf{h}_1(n+1) = \mathbf{h}_1(n) + \frac{\mu_1 e(n)}{\mathbf{x}_1^T(n)\mathbf{x}_1(n)}\mathbf{x}_1(n) \tag{4.39a}$$

$$\mathbf{h}_2(n+1) = \mathbf{h}_2(n) + \frac{\mu_2 e(n)}{\mathbf{x}_2^T(n)\mathbf{x}_2(n)}\mathbf{x}_2(n) \tag{4.39b}$$

As a result, in order to guarantee the convergence of the VF coefficients in the mean sense, we can set the following range for the step sizes,

$$0 < \mu_1 < 1 \tag{4.40a}$$

$$0 < \mu_2 < 1 \tag{4.40b}$$

which is different from the range $0 < \mu_1 < 2$ and $0 < \mu_2 < 2$ in the method [4], where the two kernels are treated independently.

As a matter of fact, it is found from computer simulations that if both μ_1 and μ_2 are larger than one, the NLMS would not converge.

4.2.2 Eigenvalue Spread Analysis of Kernel-Separated VF

It is known that the variance of the input signal would severely affect the eigenvalue spread of the correlation matrix of the input vector of a 2nd order VF, which in turn affects the convergence rate of the NLMS algorithm even if the input is a Gaussian process. In

this section , we show that the convergence of kernel-separated VFs is less sensitive to the variance of the input signal. The following investigation is based on the assumption that a Gaussian input with a zero mean and variance σ^2 is applied to the VF. We first consider that cast of separated kernels. Since the correlation matrix of the 1st order Volterra kernel is a diagonal matrix whose element is the variance σ^2, its eigenvalue spread is unity. Thus, the convergence of the 1st order kernel is not affected by the variance of the input signal.

The elements of the correlation matrix of the second-order kernel can be expressed as the following general form [36],

$$E(x_{i1}x_{i2}x_{i3}x_{i4}) = E(x_{i1}x_{i3})E(x_{i2}x_{i4}) + E(x_{i1}x_{i4})E(x_{i3}x_{i2}) + E(x_{i1}x_{i2})E(x_{i3}x_{i4}) \quad (4.41)$$

where x_{i1}, x_{i2}, x_{i3} and x_{i4} denote four delayed versions of four input samples. There are several cases for the combination of the four elements

If $x_{i1} = x_{i2} = x_{i3} = x_{i4}$,

$$E(x_{i1}x_{i2}x_{i3}x_{i4}) = \sigma^{2p}\frac{(2p)!}{(p!2^p)} = 3\sigma^4 \quad (4.42)$$

If $x_{i1} = x_{i3}, x_{i2} = x_{i4}$ and $x_{i1} \neq x_{i2}$,

$$E(x_{i1}x_{i2}x_{i3}x_{i4}) = E(x_{i1}^2 x_{i2}^2) = \sigma^4 \quad (4.43)$$

Otherwise,

$$E(x_{i1}x_{i2}x_{i3}x_{i4}) = 0 \quad (4.44)$$

Thus, we only have two non-zero values in the correlation matrix of the 2nd order kernel, denoted $a\sigma^4$,($a = 1, 3$). Accordingly, the correlation matrix of the 2nd order kernel can be represented generally

$$\mathbf{R}_2=\delta^4\begin{bmatrix} a_{00} & a_{01} & \cdots & a_{03} \\ a_{10} & a_{11} & & a_{13} \\ & \vdots & \ddots & \\ a_{30} & a_{31} & & a_{33} \end{bmatrix}=\delta^4\mathbf{R}_2' \tag{4.45}$$

where $\mathbf{R}_2'$ is a constant matrix whose element is 0, 1 or 3. Clearly, the eigenvalue spread of $\mathbf{R}_2$ equals that of $\mathbf{R}_2'$ which does not depend on the variance σ^2.

For a 2nd order VF whose kernel are not separated since correlation matrix of the input vector of the entire VF contains both the 2nd order and higher order (3rd and 4th order) statistics, it cannot be written as the form in (4.45). Therefore, its eigenvalue spread depends on the variance of the input signal. This justifies that the convergence of kernel-separated VFs is in general better than that of non-kernel-separated VFs.

4.3 Simulation Results

The echo return loss enhancement (ERLE) is employed to evaluate the performances of the proposed echo canceller in comparison to some of the existing methods. The ERLE is defined by the following equation [10]:

$$ERLE(n)(dB)=10\log 10\frac{E[d^2(n)]}{E[e^2(n)]} \tag{4.46}$$

where $d(n)$ is the desired signal picked up by the microphone and $e(n)$ is the residual echo signal after the AEC. In the simulation, the AEC system is excited with a white Gaussian noise, and a measurement noise is added to the desired signal $d(n)$ as environmental disturbance.

4.3.1 Performance of Proposed NLMS algorithm for Kernel-separated 2nd order VF

In this subsection, we will verify the performance of the proposed NLMS algorithm for kernel-separated 2nd order VF as described by equation (4.39) in comparison with a conventional NLMS algorithm directly employed in the nonlinear filter as described by equation (3.13). Figure 4.3 shows the ERLE plot of the proposed NLMS algorithm as well as the conventional one for various input signals with different variances. In this experiment, the echo path is assumed to be a 2nd order VF with 96 coefficients for the 1st order kernel and 210 coefficients for the 2nd order kernel. The echo path is identified by a same VF with unknown coefficients. In the updating process, we choose the step size μ=0.5 for the conventional NLMS algorithm, and $\mu_1 = 0.55$ $\mu_2 = 0.45$ for the 1st and the 2nd kernel, respectively, for the proposed NLMS. It is seen that when the variance of the input signal is increased from 2 to 5, the proposed algorithm performs equally well in terms of the convergence rate, whereas the convergence of the conventional NLMS becomes very slow, which can also be seen clearly from Table 4.1. These results show that the proposed NLMS algorithm is able to reduce the effect of the variation of the input signal variance.

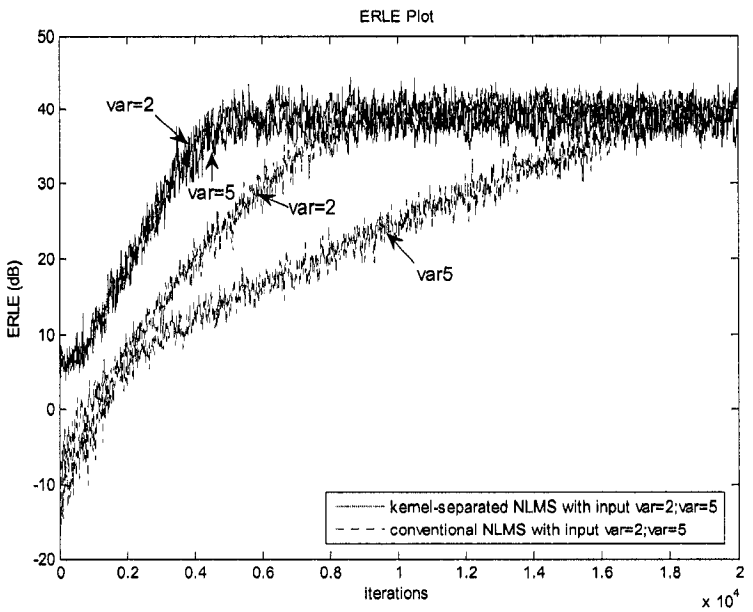

Figure 4.3 ERLE plot for input signals with different variance (Experiment 1)

Table 4.1 Convergence rate comparison of conventional NLMS and proposed NLMS

	Conventional NLMS var=2	Conventional NLMS var=5	Proposed NLMS var=2	Proposed NLMS var=5
First order kernel length (taps)	96	96	96	96
Second order kernel length (coefficients)	210	210	210	210
Convergence rate (iterations)	9000	17000	6000	6000

Figure 4.4 shows the ERLE results of both the proposed and the conventional NLMS algorithms when the echo path has a longer memory length. In this simulation, the echo path is assumed to be a 2^{nd} order VF with 128 first-order coefficients and 528 second-order coefficients. We use a VF with the same number of coefficients for both NLMS algorithms. Clearly, the convergence rate of both filters gets slower due to the increase of the number of coefficients. However, it is evident that the convergence of the proposed NLSM algorithm is much better than that of the conventional one, despite the large number of VF coefficients.

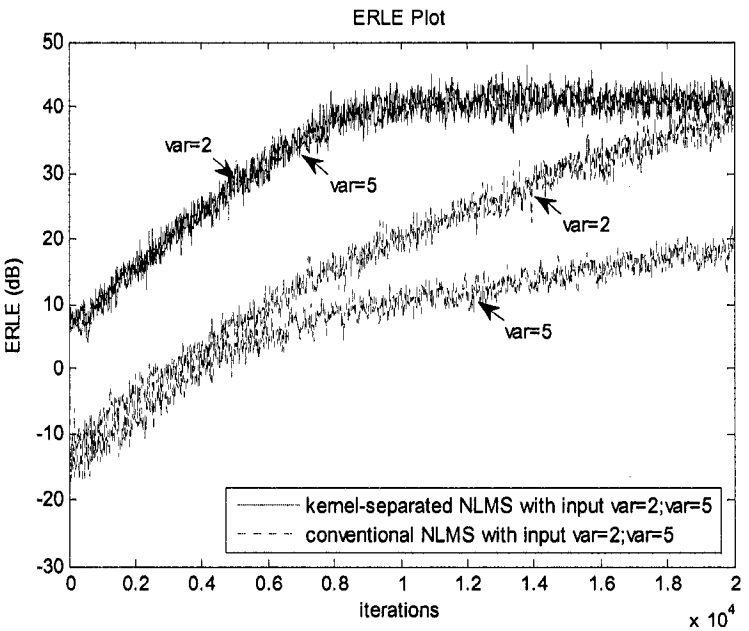

Figure 4.4 ERLE plot for input signals with different variances (Experiment 2)

It should be emphasized that the range for the step sizes μ_1 and μ_2 in the proposed NLMS algorithm has to satisfy equation (4.40). As a matter of fact, we have attempted other choices of μ_1 and μ_2 in our simulation and found that the algorithm fails to convergence when both μ_1 and μ_2 are large than 1. It should also be mentioned that in the above experiments, we used a conventional 2^{nd} order VF which has full coefficients to verify the proposed NLMS algorithm. The conclusion can also be drawn for the case of the simplified 2^{nd} order VF structure.

4.3.2 The Performance of the Simplified 2^{nd} order VF using Proposed NLMS Algorithm

In this section, the performance of the simplified 2^{nd} order VF with the proposed NLMS algorithm will be examined and compared with that of the conventional 2^{nd} order VF using the same NLMS algorithm.

Considering a real echo path is composed of a loudspeaker cascaded with the room impulse, the echo path is set to be a nonlinear cascade structure in this experiment, namely, it consists of a 2^{nd} order VF followed by an FIR filter. The 2^{nd} order VF has a memory length 64 for the first order kernel and 12 for the second order kernel. The FIR filter in the cascade structure is of 26 taps. If the nonlinear echo path is to be identified by a conventional 2^{nd} order VF, then the VF should have 89 coefficients for the 1^{st} order kernel and 703 coefficients for the 2^{nd} order kernel. However, as discussed in Chapter 4 the simplified VF with the same memory length as the conventional one has only 89 taps for the 1^{st} order kernel and 378 coefficients for the 2^{nd} order kernel. Figure 4.5 illustrates the performance of the conventional and the simplified VF. It is not surprising to see that the convergence rate of the simplified structure is faster than conventional one. As both cancellers are implemented under the same condition, we have compared their execution time. Table 4.2 gives the computational complexity comparison of both echo cancellers in terms of execution time from a Pentium PC 4 with 2 CPU 3.00 GHz and 1.00 GB RAM. It is found that the echo canceller using conventional VF is more time consuming than the simplified VF in updating process, even though both converge to the same eventual ERLE value.

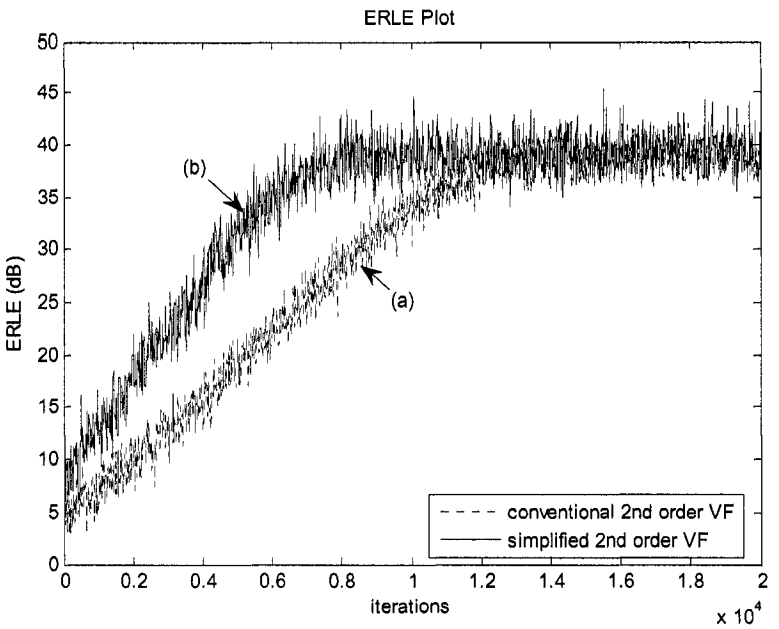

Figure 4.5 Performance comparison of two 2nd order VFs using proposed NLMS algorithm (a) conventional VF with full coefficients (b) simplified VF with reduced 2nd order kernel coefficients (Experiment 1)

Table 4.2 Comparison of two 2nd order VFs using proposed NLMS algorithm (Experiment 1)

	Conventional 2nd order VF	Simplifed 2nd order VF
First order kernel length (taps)	89	89
Second order kernel length (coefficients)	703	378
Convergence rate (iterations)	12500	9000
ERLE (dB)	40	40
Execution time/per run (seconds)	4.8	3.3

Figure 4.6 shows the results when the echo path has a longer-duration room impulse response of 32 taps. Table 4.3 shows the computational complexity of both VF structures. Clearly one can conclude that the proposed echo canceller is overall better than the conventional one in terms of convergence rate and computational complexity, even though the final ERLE value of both methods are slightly different.

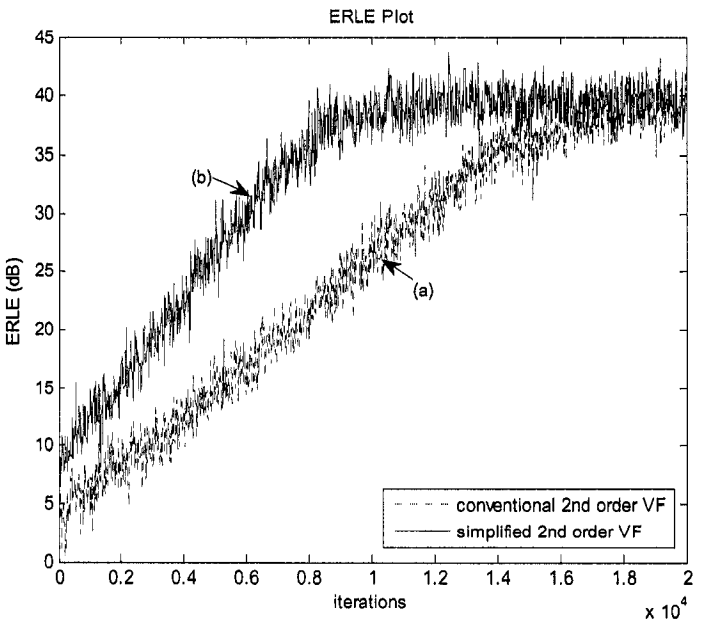

Figure 4.6 Performance comparison of two 2nd order VFs using proposed NLMS algorithm (a) conventional VF with full coefficients (b) simplified VF with reduced 2nd order kernel coefficients (Experiment 2)

Table 4.3 Comparison of two 2nd order VFs using proposed NLMS algorithm (Experiment 2)

	Conventional 2nd order VF	Simplifed 2nd order VF
First order kernel length (taps)	95	95
Second order kernel length (coefficients)	946	450
Convergence rate (iterations)	18000	10000
ERLE (dB)	38	39
Execution time/per run (seconds)	5.7	3.7

The performance of the proposed echo canceller has been investigated in the above two experiments given white Gaussian noise as the input signal. We now look into the performance of the proposed method in comparison with the conventional VF as well as the cascade VF structure as shown in Figure 3.4, when the input signal is a colored Gaussian noise. In the cascade VF structure canceller, the 2nd order VF and the FIR filter have the same number of coefficients as the echo path but with unknown parameters. Figure 4.7 shows ERLE plot of the three methods, where the parameters of the echo path

are the same as that in Figure 4.5. It is easy to see that the proposed echo canceller has the best performance while the cascade structure gives the worst ERLE due to its convergence to the local minima. It is also seen the conventional VF has a slightly worse ERLE compared to the simplified VF.

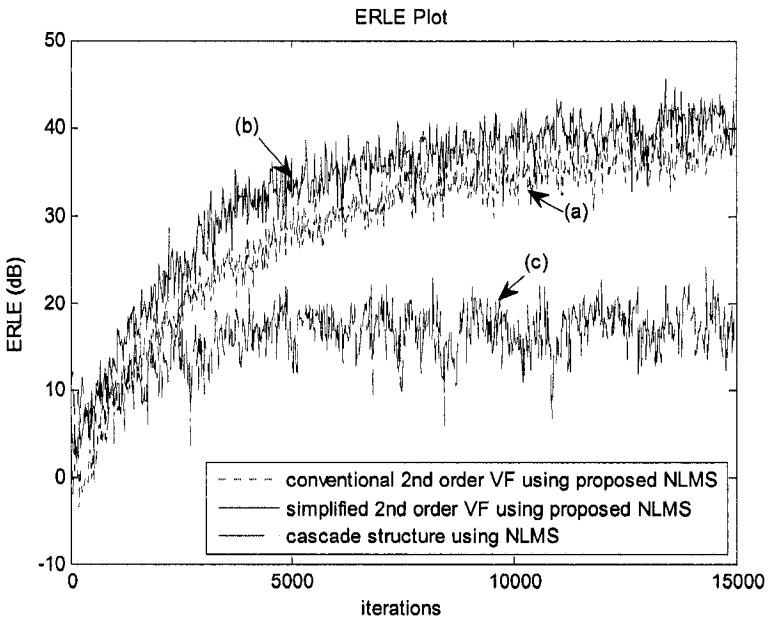

Figure 4.7 Performance comparison (a) conventional VF using proposed NLMS (b) simplified VF using proposed NLMS (c) cascade VF structure using NLMS

4.3.3 Performance of the Simplified VF using RLS Algorithm

In this section, the RLS algorithm is applied to update the coefficients of both conventional and simplified 2^{nd} order VFs. The echo path is also modeled by a cascade structure, where the 2^{nd} order VF is assumed to have 32 taps for the 1^{st} order kernel and memory length of 8 for the second order kernel. The FIR filter in the cascade structure assumed to have 14 taps. Figure 4.8 illustrates the performance of both VFs using RLS algorithm along with that of the simplified VF employing the proposed NLMS algorithm when the input is white Gaussian noise. Table 4.4 gives a comparison of the three echo

cancellers with their execution time. It is seen that the two cancellers using the RLS in general give a faster convergence than the VF using the proposed NLMS. However, the simplified VF with NLMS has a much less computational complexity than the RLS in view of the execution time. This is because the inversion of the matrix $R_D(n)$ required in RLS algorithm is very time consuming. It is also clear that the simplified VF with RLS is significantly better than conventional VF with RLS in computational complexity although both of them have the almost same convergence rate. Overall, the simplified VF structure with the proposed NLMS algorithm is a very good compromise in terms of both the convergence rate and the computational complexity.

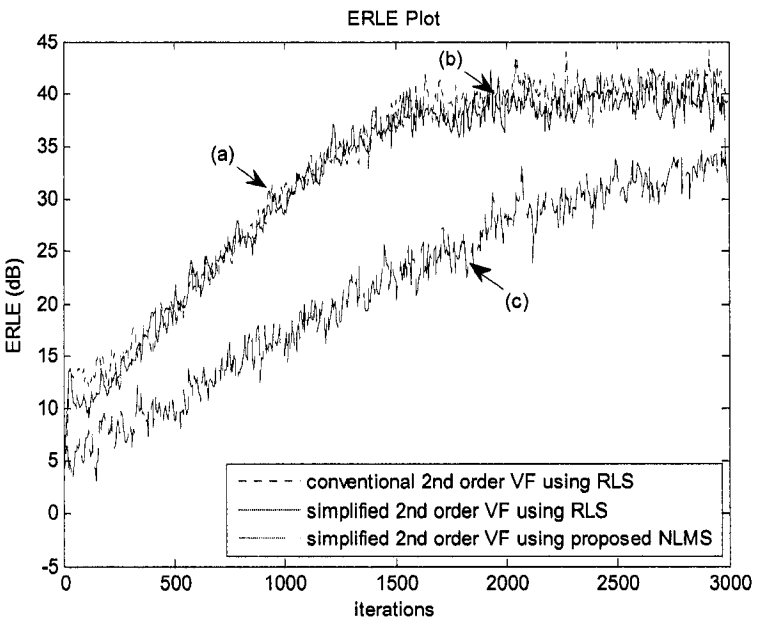

Figure 4.8 Performance comparison of 2nd order VFs using RLS and proposed NLMS (a) conventional VF using RLS (b) simplified VF using RLS (c) simplified VF using proposed NLMS

Table 4.4 Comparison of 2nd order VFs using RLS and proposed NLMS algorithms

	Conventional 2nd order VF using RLS	Simplifed 2nd order VF using RLS	Simplifed 2nd order VF using proposed NLMS
First order kernel length (taps)	45	45	45
Second order kernel length (coeffs)	231	140	140
Convergence rate (iterations)	2000	2000	>3000
ERLE (dB)	40	40	35
Execution time/per run (seconds)	15.6	5.5	0.33

Chapter 5 Nonlinear AEC Based on Sigmoid Transform and RLS Algorithm

It is known that a VF has, in general, a high computational complexity due to the involvement of a large number of filter coefficients, especially in case of large memory length and high orders. In this chapter, we propose to use a sigmoid transform to model the saturation-type nonlinear distortion. The echo canceller structure constituted by a nonlinear transform implementing a variable saturation curve and an FIR filter has been attempted by several researchers in [8], [31], [32]. In particular, the acoustic echo path is modeled as a cascade of a memoryless amplitude-limited saturation curve and a linear filter in [8], where a three-stage cascade structure is employed. Since only one adaptable parameter, namely, the maximum value of the saturation curve is used in this cascade structure, the shape of the saturation curve remains non-adjustable. Obviously, this model with only one free parameter cannot be adapted to an arbitrary shape of nonlinear distortions. In [31], the cascaded stages have been reduced to two, leading to a low-complexity echo canceller. But this method is only suitable for the ideal hard-clipping distortion, which also limits the AEC performance. More recently, a raised-cosine-function-based model has been studied in [32]. The nonlinear characteristic of the acoustic echo path is approximated by a transform that is derived from the raised-cosine function. This model is able to adapt to both soft-clipping and hard-clipping nonlinearities, and

gives a superior performance compared to the VF approaches in some situations [32]. Another advantage of this method is its low computational complexity since only two free parameters are involved in the nonlinear function and their update can easily be implemented by the derived closed-form expression. On the other hand, due to the nature of the piece-wise defined nonlinear function it seems very difficult to theoretically justify the convergence of the algorithm.

In this chapter, a new nonlinear AEC employing the sigmoid function is developed. Section 5.1 presents the detailed system model based on the nonlinear sigmoid transform as well as the update schemes for the transform parameters and the transversal filter coefficients. Section 5.2 gives the theoretical analysis of the convergence behaviour of the new echo canceller. A detailed simulation study validating the effectiveness of the proposed acoustic echo canceller is carried out in Section 5.3 with comparison to some of the existing techniques.

5.1 Proposed Acoustic Echo Canceller

The proposed adaptive nonlinear echo canceller is shown in Figure 5.1, in which the signal from a far-end user is first nonlinearly distorted by the amplifier/loudspeaker and then passed through the linear echo path characterized by the room impulse response. Note that the nonlinear distortion is assumed to be of saturation type but with unknown parameters. In order to compensate for the nonlinearity of the amplifier/loudspeaker in the complete echo path, a nonlinear transform implementing the saturation curve with adaptable free parameters is used. Clearly, the adaptive transversal filter is employed to cancel the effect of the room impulse response of the echo path. In this paper, we adopt the following two-parameter sigmoid function [14] for the nonlinear transform.

$$f(x) = \frac{2\beta}{1+\exp(-\alpha\ x)} - \beta \tag{5.1}$$

where α and β determine, respectively, the shape and the clipping value of the saturation curve. This function can accurately cover a large range of nonlinear distortions by choosing different values of α and β. Although the parameter β could be easily removed from equation (5.1) by combining it with the weight vector of the subsequent linear adaptive filter in the AEC, it is advantageous to keep in the nonlinear transform since it can mimic the actual dynamic range of the amplifier. It should be mentioned that even though the sigmoid function has been utilized in [8], [31], its capability of fitting a variable saturation curve was not well exploited. Our idea in this chapter is to update the two parameters α and β by using the LMS algorithm such that the unknown nonlinear distortion of the amplifier is best matched, thereby cancelling the nonlinear component in the echo path.

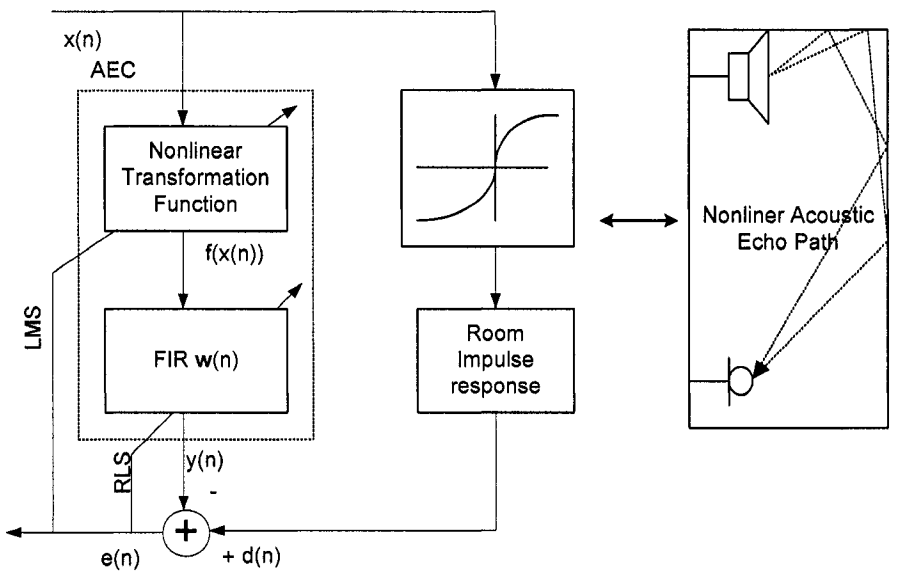

Figure 5.1 Proposed nonlinear acoustic echo canceller

Denote the input signal vector of length L by $\mathbf{x}(n)$, and the estimate output signal of the linear adaptive filter by y(n).

$$y(n)=\mathbf{w}^T(n)\, f(\mathbf{x}(n)) \tag{5.2}$$

where $\mathbf{w}(n)$ represents the coefficient vector of the transversal filter, and $f(\mathbf{x}(n))=[f(x(n)),\ f(x(n-1)),\ \cdots,\ f(x(n-L+1))]^T$ is the nonlinearly transformed vector corresponding to $\mathbf{x}(n)$. Then, the estimated error $e(n)$ can be expressed as

$$e(n)=d(n)-y(n)=d(n)-\mathbf{w}^T(n)f(\mathbf{x}(n)) \tag{5.3}$$

where $d(n)$ is the desired signal which is the echo collected by the microphone. From equation (5.3), we can calculate the mean-square-error (MSE) $J(n)$ as

$$J(n)=E[e^2(n)]=E[(d(n)-\mathbf{w}^T(n)f(\mathbf{x}(n)))^2] \tag{5.4}$$

In equation (5.4), there are three unknown parameters, α, β and $\mathbf{w}(n)$. The LMS algorithm is used to determine the optimal solution of α and β, leading to the following update formulas.

$$\alpha_{n+1}=\alpha_n-\frac{\mu_\alpha}{2}\hat{g}_\alpha(n) \tag{5.5}$$

$$\beta_{n+1}=\beta_n-\frac{\mu_\beta}{2}\hat{g}_\beta(n) \tag{5.6}$$

where $\hat{g}_\alpha(n)$ and $\hat{g}_\beta(n)$ represent the estimate of the gradient of $J(n)$ with respect to α and that to β, respectively. Substituting equation (5.4) into equations (5.5) and (5.6) respectively, gives

$$\alpha_{n+1}=\alpha_n-\frac{\mu_\alpha}{2}\hat{g}_\alpha(n)=\alpha_n-\frac{\mu_\alpha}{2}\frac{\partial J(n)}{\partial\alpha}\Big|_{\beta=\beta_n}=\alpha_n+\mu_\alpha e(n)\mathbf{w}^T(n)\frac{\partial f(\mathbf{x}(n))}{\partial\alpha}\Big|_{\beta=\beta_n} \tag{5.7}$$

where each element of $\frac{\partial f(\mathbf{x}(n))}{\partial\alpha}$ is given by

$$\frac{\partial f(x)}{\partial \alpha} = \frac{2x\exp(-\alpha\ x)}{(1+\exp(-\alpha\ x)^2}\beta \tag{5.8}$$

and

$$\beta_{n+1} = \beta_n - \frac{\mu_\beta}{2}\hat{g}_\beta(n) = \beta_n - \frac{\mu_\beta}{2}\frac{\partial J(n)}{\partial \beta}\Big|_{\alpha=\alpha_n} = \beta_n + \mu_\beta e(n)\mathbf{w}^T(n)\frac{\partial f(\mathbf{x}(n))}{\partial \beta}\Big|_{\alpha=\alpha_n} \tag{5.9}$$

where each element of $\frac{\partial f(\mathbf{x}(n))}{\partial \beta}$ is given by

$$\frac{\partial f(x)}{\partial \beta} = \frac{2}{1+\exp(-\alpha x)} - 1 \tag{5.10}$$

It is to be noted that equations (5.8) and (5.10) are obtained by using each sample of the input vector $\mathbf{x}(n)$ to the function $f(x)$. μ_α and μ_β represent the convergence factors, which determine the step size in the update of α and β.

In this paper, we adopt the RLS algorithm to update the weight vector **w**(n) of the transversal filter due to its fast convergence speed. Here, we assume that the input signal vector of the transversal filter is defined by $\mathbf{u}(n)$, which can be formulated by $\mathbf{u}(n) = [f(x(n)), f(x(n-1)), f(x(n-2)), \cdots f(x(n-L+1))]^T\Big|_{\alpha=\alpha_n,\beta=\beta_n}$ with L being the length of the transversal filter. The RLS algorithm is briefly described as follows [12].

Initialization

$$\mathbf{S}_D(n-1) = \delta I$$

$$\mathbf{x}(-1) = \mathbf{w}(-1) = [0 \quad 0 \quad \cdots \quad 0]^T$$

Do for $n \geq 0$

$$e_{pri}(n) = d(n) - \mathbf{u}^T(n)\mathbf{w}(n-1) \tag{5.11}$$

$$\psi(n) = \mathbf{S}_D(n-1)\mathbf{u}(n) \tag{5.12}$$

$$\mathbf{S}_D(n) = \frac{1}{\lambda}[\mathbf{S}_D(n-1) - \frac{\psi(n)\psi^T(n)}{\lambda + \psi(n)\mathbf{u}(n)}] \tag{5.13}$$

$$\mathbf{w}(n) = \mathbf{w}(n-1) + e_{pri}(n)\mathbf{S}_D(n)\mathbf{u}(n) \tag{5.14}$$

---

where λ with $0 << \lambda < 1$ is the forgetting factor and δ a small constant determining the initial matrix which can be chosen as the inverse of an estimate of the input signal power of the FIR filter. Note that the update of α, β and $\mathbf{w}(n)$ is on sample-by- sample basis. For each input sample, these parameters are updated once. As seen from equations (5.7) and (5.9), the old values of α and β from the last iteration should be used when updating α and β for the current iteration.

5.2 Convergence Analysis

The nonlinear characteristic of the transform makes an accurate theoretical analysis of the convergence of the proposed AEC rather complicated and difficult [12], [30]. In this section, we provide a convergence analysis under some assumptions, including the independence assumptions well-described in [14],

- The input vectors $\mathbf{x}(1)$, $\mathbf{x}(2)$,..., $\mathbf{x}(n)$ are a set of statistically independent vectors.
- At any time n, the input vector $\mathbf{x}(n)$ is statistically independent of all previous desired signals $d(1)$, $d(2)$,..., $d(n-1)$.
- At any time n, $d(n)$ is just dependent on the corresponding input vector $\mathbf{x}(n)$ but statistically independent of all previous samples of the desired signals.

According to the independence assumption, the input $x(n)$, the intermediate signal $f(x(n))$ and the output $y(n)$, as described in the Figure 5.1, are all wide-sense stationary (WSS) processes.

Assume that the unknown nonlinear echo system is described by $\hat{\alpha}$, $\hat{\beta}$ and $\mathbf{w}_0$, where $\mathbf{w}_0$ is to be identified by the proposed adaptive FIR filter of the same order. As $\hat{\beta}$ can readily be combined with $\mathbf{w}_0$ as a new $\mathbf{w}_0$, the convergence analysis is thus simplified to the study of α and $\mathbf{w}$.

5.2.1 Convergence of the Sigmoid Parameter

The error of α_n at the *nth* iteration can be written as

$$\Delta\alpha_n = \alpha_n - \hat{\alpha} \tag{5.15}$$

Using equation (5.7), we have

$$\Delta\alpha_{n+1} = \Delta\alpha_n + \mu_\alpha e(n)\mathbf{w}^T(n)\frac{\partial f(\mathbf{x}(n))}{\partial\alpha} \tag{5.16}$$

where,

$$e(n) = \mathbf{w}_0^T\left(\frac{2}{1+\exp(-\hat{\alpha}\mathbf{x}(n))} - 1\right) - \mathbf{w}^T(n)\left(\frac{2}{1+\exp(-\alpha_n\mathbf{x}(n))} - 1\right) \tag{5.17}$$

We now expand the function $f(x)$ given by equation (5.1) as a Taylor series with respect to $\hat{\alpha}$. As β has been combined with the FIR coefficients, a series expansion can be obtained as follow [37].

$$\begin{aligned} f_{\hat{\alpha}}(\alpha_n) &= f(\hat{\alpha}) + f'(\hat{\alpha})(\alpha_n - \hat{\alpha}) + \{higher\ \ order\ \ terms\} \\ &= f(\hat{\alpha}) + f'(\hat{\alpha})\Delta\alpha_n + \{higher\ \ order\ \ terms\} \end{aligned} \tag{5.18}$$

where $f'(\cdot)$ represents the first order derivative, and the higher order items can be ignored [37]. Using equation (5.18) into (5.17) and then substituting the result into (5.16) and assuming that $\mathbf{w}(n) \to \mathbf{w}_0$ as $n \to \infty$, we have

$$\Delta\alpha_{n+1} \approx \Delta\alpha_n + \mu_\alpha \mathbf{w}_0{}^T [-\frac{\partial f(\mathbf{x}(n))}{\partial \alpha}\Big|_{\alpha=\hat{\alpha}} (\alpha_n - \hat{\alpha})] \mathbf{w}_0{}^T \frac{\partial f(\mathbf{x}(n))}{\partial \alpha}$$

$$= \Delta\alpha_n [1 - \mu_\alpha \mathbf{w}_0^T \frac{\partial f(\mathbf{x}(n))}{\partial \alpha}\Big|_{\alpha=\hat{\alpha}} \mathbf{w}_0^T \frac{\partial f(\mathbf{x}(n))}{\partial \alpha}\Big|_{\alpha=\alpha_n}] \tag{5.19}$$

where

$$\frac{\partial f(\mathbf{x}(n))}{\partial \alpha} = [f'(x(n)) \quad f'(x(n-1)) \quad \cdots \quad f'(x(n-L+1))]^T \tag{5.20}$$

with $f'(x(n)) = \frac{2x(n)\exp(-\alpha x(n))}{(1+\exp(-\alpha x(n)))^2}$ and L being the length of the FIR filter.

For the sake of simplicity, let

$$v_\alpha(n) = \mathbf{w}_0{}^T \frac{\partial f(\mathbf{x}(n))}{\partial \alpha} \tag{5.21}$$

Then, equation (5.19) can be rewritten as,

$$\Delta\alpha_{n+1} \approx \Delta\alpha_n [1 - \mu_\alpha v_{\hat{\alpha}}(n) v_{\alpha_n}(n)] \tag{5.22}$$

where $v_{\hat{\alpha}}(n)$ represents the estimate of $v_{\alpha_n}(n)$. By further assuming that $v_{\hat{\alpha}}(n)$ is WSS and $v_{\alpha_n}(n)$ approximates closely $v_{\hat{\alpha}}(n)$ when n is large, the expectation of the error in (5.22) can be calculated

$$E(\Delta\alpha_{n+1}) = (1 - \mu_\alpha r_v(0)) E(\Delta\alpha_n)$$

$$= [1 - \mu_\alpha r_v(0)]^{n+1} E(\Delta\alpha_0) \tag{5.23}$$

where $r_v(0)$ is the autocorrelation of the process $v_{\hat{\alpha}}(n)$. It is seen from equation (5.23) that when $-1 < 1 - \mu_\alpha r_v(0) < 1$, namely $0 < \mu_\alpha < 2/r_v(0)$, $E(\Delta\alpha_{n+1})$ tends to zero as $n \to \infty$.

5.2.2 Convergence of the Coefficient Vector

We now conduct the convergence analysis of the linear filter coefficient vector $\mathbf{w}(n)$ in the proposed AEC based on the WSS assumption made at the beginning of this section. The system input signal $x(n)$, the output signal $f(x(n))$ of the nonlinear transfer function and the output of the whole system y(n), as described in the Figure 5.1, are assumed to be wide sense stationary(WSS) processes. Our objective is show that the derived LS solution approaches the ideal Wiener solution.

Assume that a measurement noise $n_0(n)$ is added to the desired signal, leading to

$$d(n) = \mathbf{w}_0{}^T f(\mathbf{x}(n)) + n_0(n) \tag{5.24}$$

where $\mathbf{w}_0$ is the ideal coefficients which are to be identified by the proposed adaptive filter of the same order. The additional noise $n_0(n)$ is considered to be an AWGN with zero mean and variance $\delta_n{}^2$. From [12], when $\lambda = 1$ we can get

$$\begin{aligned}\mathbf{w}(n) &= R_D^{-1}(n)P_D(n) \\ &= \left[\sum_{i=0}^{n} \lambda^{n-i} f(\mathbf{x}(i)) f^T(\mathbf{x}(i))\right]^{-1} \sum_{i=0}^{n} \lambda^{n-i} f(\mathbf{x}(i)) d(i) \\ &= \left[\sum_{i=0}^{n} f(\mathbf{x}(i)) f^T(\mathbf{x}(i))\right]^{-1} \sum_{i=0}^{n} f(\mathbf{x}(i)) d(i)\end{aligned} \tag{5.25}$$

Supposing that the $f(x(n))$ is WSS, from the first part of equation (2.25), we can obtain

$$\lim_{n\to\infty} \frac{1}{n+1} \sum_{i=0}^{n} f(\mathbf{x}(i)) f^T(\mathbf{x}(i)) = \mathrm{R} \tag{5.26}$$

where R is the correlation matrix of the input signal of the FIR filter. Using equations (5.24) and (5.26) and considering additive noise is independent of the input signal of the linear part, we can get,

$$\lim_{n\to\infty}\frac{1}{n+1}\sum_{i=0}^{n} f(\mathbf{x}(i))d(i) = \lim_{n\to\infty}\frac{1}{n+1}\sum_{i=0}^{n} f(\mathbf{x}(i))(f^T(\mathbf{x}(i))\mathbf{w}_0 + n_0(i))$$

$$= \lim_{n\to\infty}\frac{1}{n+1}\sum_{i=0}^{n} f(\mathbf{x}(i))f^T(\mathbf{x}(i))\,\mathbf{w}_0$$

$$= \mathbf{R}\,\mathbf{w}_0 \tag{5.27}$$

when n is very large, using equations (5.26) and (5.27) into equation (5.25) gives

$$\mathbf{w}(n) = R_D^{-1}(n)P_D(n) = R^{-1}R\mathbf{w}_0 = \mathbf{w}_0 \tag{5.28}$$

This result indicates that the least-squares solution of **w** turns to the Wiener solution as long as the signals involved are ergodic and stationary.

5.3 Simulation Results

As usual, the echo return loss enhancement (ERLE) is employed to evaluate the performances of the proposed method in comparison with some of the existing methods. For understanding easily, here, we briefly introduce the concept of the ERLE again:

$$ERLE(n)(dB) = 10\log 10\frac{E[d^2(n)]}{E[e^2(n)]} \tag{5.29}$$

where $d(n)$ is the desired signal picked up by the microphone and $e(n)$ is the residual echo signal after the echo cancellation. In the following simulations, the AEC system is excited with a white Gaussian noise, and a measurement noise is added to the desired signal $d(n)$ as environmental disturbance. We would like to examine the convergence behavior of parameters α and β and the ERLE performance of the proposed method along with that of the linear canceller and the Volterra filter-based canceller.

5.3.1 Learning Curve of the Nonlinear transform

To demonstrate the capability of the proposed sigmoid transform in adaptation to different distortion situations, we assume three pairs of values for (α, β), namely, (6, 3.5), (4, 3), and (1.5, 1), for the simulation study. These choices represent three typical nonlinear distortions as shown in Figure 5.2 (a). The learning curves of α and β are examined for these nonlinear transforms. To evaluate the tracking ability in noisy environment, a measurement noise is added in the simulation. Through extensive simulations, we find the convergence speed of α and β is dictated mainly by the step size of the update mechanism and μ=0.05~0.15 is a proper choice for the update of both parameters in view of both the convergence speed and the misadjustment. Figure 5.2 (b) and (c) give the learning curve of α and that of β, respectively, for the three distortion cases when μ=0.1. From Figure 5.2(a), (b) and (c), it is clear that both parameters can always converge to the true values very fast with little misadjustment in all the distortion cases, and a higher-order nonlinearity has a little bit slower convergence. It proves that this sigmoid method is suitable for nonlinear distortion adaptation.

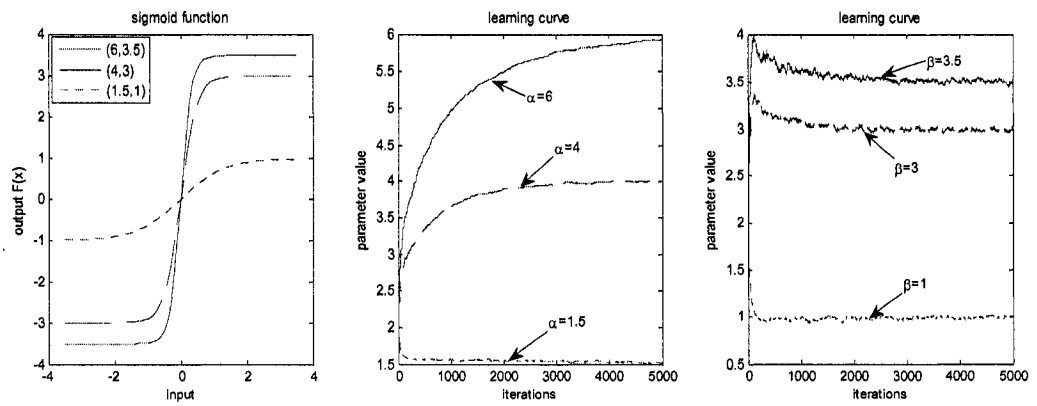

(a) (b) (c)

Figure 5.2 Convergence behavior of Sigmoid function, (a) three typical saturation-type distortions, (b) learning curves of α, (c) learning curve of β

5.3.2 ERLE of the Proposed AEC with Comparisons

In all the following simulations, big step size of α and β maybe make the updating speed faster, it also causes the unstable problem, so the updating step size of α and β should be chosen carefully. To make sure the stable results, in this section, the step sizes of α and β are always chosen less than 0.15 and the forgetting factor value of RLS is above 0.995. Figure 5.3 shows the ERLE of the proposed canceller in comparison with that of the NLMS based linear filter. In this experiment, the echo path is modeled by a saturation curve with parameters $\hat{\alpha}$=4, $\hat{\beta}$=3 and a 128-tap linear filter. The echo path is identified by the new nonlinear method as well as the conventional linear NLMS algorithm, both of which use a 128-tap transversal filter with unknown coefficients. It is not surprising that the proposed canceller performs much better than the conventional linear echo canceller, since the nonlinear echo component cannot be compensated by a linear FIR filter.

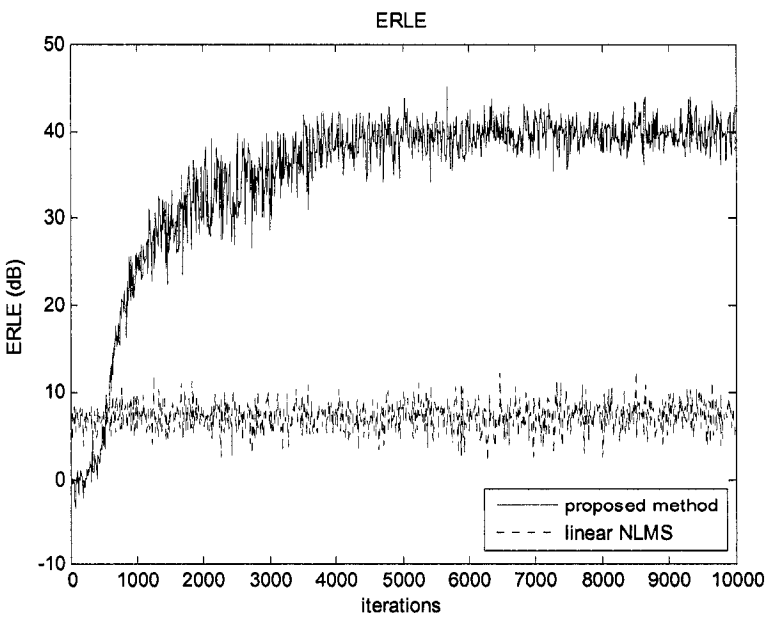

Figure 5.3 ERLE comparison with linear NLMS filter

Figure 5.4 compares the ERLE performance of the proposed nonlinear filter with that of a truncated 2nd order VF [10]. The echo path is the same as that in Figure 5.3, but the room impulse response is now assumed to be 64-tap long. The nonlinear VF canceller consists of a 64 linear coefficients and a 210 nonlinear coeffients. For avoiding the false convergence caused by RLS algorithm, the parameters of the proposed method is always fixed when a threshold is reached, such as error less than a small ξ value. We can see from Figure 5.4 that the ERLE has no big changes after the parameters are fixed. It proves that the proposed method makes the updating parameters converge to the values which are close to the true ones. We can also obtain that the proposed method converges fast to the true echo channel and gives a much better ERLE value than the 2nd order VF does.

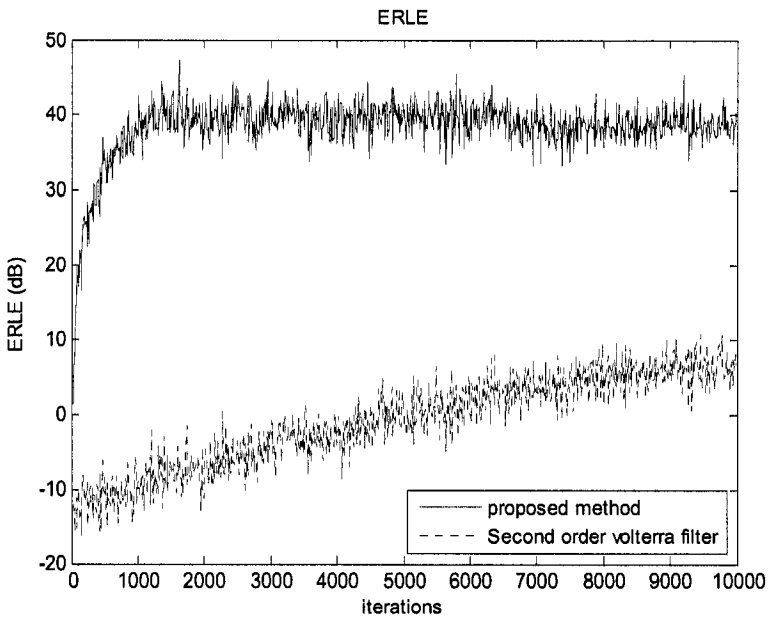

Figure 5.4 ERLE comparison with a second order VF

The proposed nonlinear echo canceller is also evaluated in the linear distortion situation. In Figure 5.5, the simulation echo path is modeled by two 64-taps transversal filters in conjunction. Both AECs in last simulation are also used to do comparison, it can

be seen that the ERLE performance of the NLMS 2nd order VF is better than that of the proposed method. But we can see the proposed echo canceller can also reach an acceptable performance. It is because the sigmoid function is not competent in approximating a linear mapping. Finally Figure 5.6 depicts the simulation results when the nonlinear echo path is modeled by a 3rd order VF with 64-tap linear response, and 55 coefficients for the 2nd order and 35 coefficients for the 3rd order nonlinear parts. As shown, the ERLE result is in favour of the 2nd order VF, suggesting that a VF, rather than the sigmoid function-based canceller, be employed if the echo path is of a nonlinear nature that is described by a nonlinear polynomial with memory and cross terms. It is worth mentioning that in all the above situations, the proposed nonlinear canceller always exhibits a fast convergence.

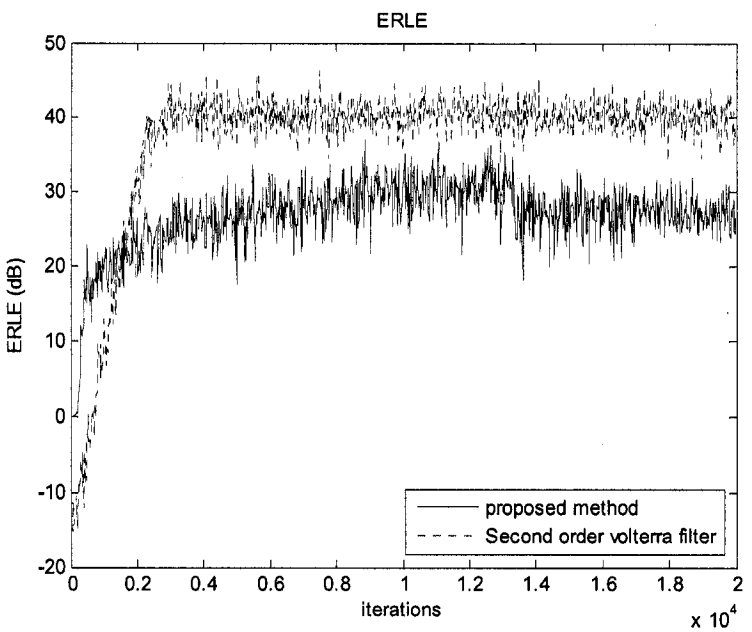

Figure 5.5 ERLE comparison with second order VF for a linear echo path

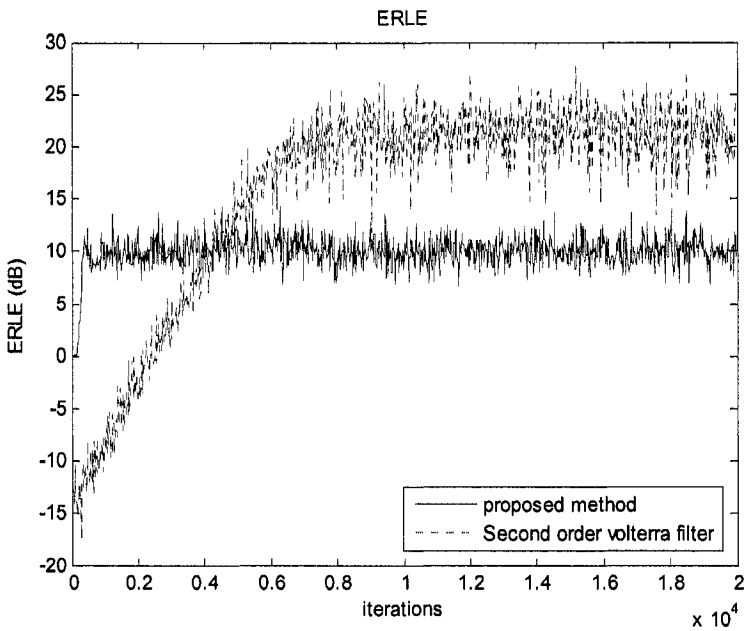

Figure 5.6 ERLE comparison with 2nd order VF for the echo path modeled by a 3rd order VF

Chapter 6 Conclusion

6.1 Concluding Remarks

The objective of this thesis has been to develop efficient nonlinear adaptive filter structures and algorithms for the cancellation of acoustic echo signals in loudspeaker and amplifier systems used in hands-free telephones or teleconferences. Due to the diverse characteristics of nonlinearities caused by loudspeaker and amplifier, two kinds of acoustic echo cancellers for different nonlinear situations have been proposed and analyzed.

To cancel the nonlinearity caused mainly by a loudspeaker, we have employed a 2^{nd} order VF. By comparing a general 2^{nd} order VF with a cascade structure of a 2^{nd} order VF plus a linear filter, we have proved that the cascade structure can be equivalently converted to a simplified 2^{nd} order VF with reduced coefficients for the 2^{nd} order kernel. A NLMS algorithm for kernel-separated 2^{nd} order VF was also derived to speed up the update of the Volterra kernel coefficients. A new convergence factor has also been obtained for the proposed NLMS algorithm. It has been verified by computer simulations that the proposed simplified 2^{nd} order VF using the new NLMS algorithm has less computational complexity and faster convergence rate than a conventional 2^{nd} order VF. Extensive simulation results have also shown that the derived NLMS algorithm for kernel-separated 2^{nd} order VF with new step size range is less sensitive to the input signal

variance than the conventional NLMS algorithm. Furthermore, the superiority of the simplified 2nd order VF has also been demonstrated via the RLS algorithm which was used to update the coefficients of the nonlinear filter.

For modeling a nonlinear acoustic system without memory, we have proposed a simple yet fast-converging AEC which consists of a sigmoid function-based transform and a conventional linear adaptive filter. The update mechanism of the transform parameters and the adaptive filter coefficients has been investigated according to the LMS and RLS algorithms. A theoretical justification of the convergence of the new method has also been presented. It has been shown through an intensive simulation study that the proposed method outperforms the VF approach when the echo path undergoes a saturation-type nonlinear distortion, while the proposed method has a much faster convergence in all the distortion cases of the echo path. The simulation results have indicated that the performance of a nonlinear echo canceller depends to a large degree on the distortion nature of the echo path.

6.2 Future work

This thesis proposed two kinds of nonlinear acoustic echo cancellers, a simplified 2nd order VF-based canceller and a sigmoid transform-based RLS canceller. The proposed simplified 2nd order VF and NLMS algorithm exhibit superior performance to conventional 2nd order VF. However, the AECs based on the 2nd order VF have its limit in cancelling higher-order nonlinear distortion. Recent studies have shown the benefits of using higher-order VF which can model higher-order nonlinear distortions. Hence, one could extend the proposed simplification strategy to higher-order VFs to develop new nonlinear AECs.

The sigmoid transform-based canceller has been proved to be suitable for the cancellation of acoustic echo in some specific nonlinear situations. The further research, however, is warranted to discover other transforms which can cover a wider range of saturation curves including hard-clipping, soft-clipping and linear distortions, yet have relatively simple forms. AECs using new transforms to compensate the distortion of an amplifier might outperform the proposed canceller.

Usually, the human voice is stationary for a short period. Which means the speech turns to be non-stationary over a long period. However, in this thesis, the proposed AECs use the white Gaussian noise as input signal to evaluate their ERLE performances, which is certainly an ideal case. Hence, in order to confirm the improved performance of the proposed AECs for real speech communications, it is necessary to carry out experiments for the nonlinear echo canceller under the input of real speech data.

References:

[1] F. A. Westall and S. F. A. lp. Digital signal processing in telecommunications, London; New York: Chapman&Hall, 1993.

[2] M. M. Sondhi, "The history of echo cancellation," IEEE Signal Processing Magazine, vol. 23, no. 5, pp: 95-102, Sept. 2006.

[3] X. J. Lu, "Acoustic echo cancellation over nonlinear channels," Ph.D dissertation, McGill University, Canada, 2004.

[4] A. Stenger and R. Rabenstein, "Adaptive Volterra filters for nonlinear acoustic echo cancellation," Proc. NSIP'99 Antalya, Turkey, pp.679-683, Jun. 1999.

[5] Arie J. M. Kaizer, "Modeling of the nonlinear response of an electrodynamic loudspeaker by a volterra series expansion," J. Audio Eng. Soc., vol. 35, no. 6, pp. 421-433, June 1987.

[6] A. J. M. Kaizer, "Modeling of the nonlinear response of an electrodynamic loudspeaker by a volterrra series expansion," J. audio Eng. Soc., vol. 35, no. 6, pp. 421-433, 1987.

[7] A. Stenger and R. Rabenstein, "An acoustic echo anceller with compensation of nonlinearties," Proc. EVSIPCO'98, Isle of Rhods, Greece, pp. 969-972, Sept. 1998.

[8] B. S. Nollett and D. L. Jones, " Nonlinear echo cancellation for hands-free speakerphones," in Proc. NSIP, Mackinac Island, MI, Sept. 1997.

[9] S. Kulakcherla "Nonlinear adaptive filter for echo cancellation of speech coded signals," Master thesis, University of Missouri-Columbia, 2004.

[10] A. Fermo, A. Carini and G. Sicuranza, "Analysis of different low complexity nonlinear filters for acoustic echo cancellation," Proc. of the first international workshop (IWISPA'00), pp: 261-266, June 14-15, 2000.

[11]B. Widrow and S. D. Stearns. Adaptive signal processing, Englewood Cliffs, N. J. Prentice-Hall, 1985.

[12] P.S.R Diniz, Adaptive filtering, second edition, Kluwer Academic Publishers, 2002.

[13] D. R. Morgan, "Slow asymptotic convergence of LMS acoustic echo cancellers," IEEE Trans. Speech and Audio Processing, vol. 3, no. 2, pp: 126-136, march. 1995.

[14] S. Haykin, Adaptive Filter Theory. Upper Saddle River, NJ: Prentic-Hall, 2002.

[15] S. Makino and Y. Kaneda, "Acoustic echo canceller algorithm based on the variation characteristics of a room impulse response," ICASSP'90, vol. 2, pp: 1133-1136, 3-6 April 1990.

[16]A. Tandon, M. O. Ahmad and M. N. S. Swamy, "An efficient, low-complexity, normalized LMS algorithm for echo cancellation," NEWCAS 2004, pp: 161-164, 20-23 June 2004.

[17] A. Gilloire, T. Petillon and S. Theodoridis, "Acoustic echo cancellation using fast RLS adaptive filters with reduced complexity," ISCAS'92, vol 4, pp: 2065-2068, 3-6 may 1992.

[18] T. Petillon, A. Gilloire and S. Theodoridis, "Complexity reduction in fast RLS transversal adaptive filters with application to acoustic echo cancellation," ICASSP'92, vol. 4, pp: 37-40, 23-26 march 1992.

[19] J. M. cioffi, "Limited precision effects in adaptive filtering," IEEE Trans. On circuits and systems, vol. CAS-34, pp. 821-833, Jul. 1987.

[20] X. Li, "Fast algorithms for Volterra-series-based nonlinear adaptive filters," Ph.D dissertation, University of Illinois at Urbana-Champaign, 1998.

[21] F. X. Y. Gao and W. M. Snelgrove, "Adaptive linearization of a loudspeaker," IEEE ICASSP'91, vol. 5, pp. 3589-3592, April 1991.

[22] E. J. Thomas, "Some considerations on the application of the Volterra representation of nonlinear networks to adaptive echo canceller," Bell systems Technical Journal. vol. 50, no. 8, pp. 2797-2905, Oct. 1971.

[23] W. Frank, R. Reger and U. Appel, "Loudspeaker nonlinearities-analysis and compensation," Asilomar Conference on Signals, Systems and Computers (ACSSC), vol. 2, pp.756-760, 26-28 Oct. 1992.

[24] T. Ishikava. Et al., Trans. of IEICEA, vol. J79-A, no.7, pp. 1236-1243, Jul. 1996.

[25] M. Schetzen, The Volterra and Wiener Theories of Nonlinear systems. New York: Krieger, Florida, 1989.

[26] M. Tsujikawa, t. Shiozaki, Y. Kajikawa and Y. Nomura, "Identification and elimination of second-order nonlinear distortion of loudspeaker systems using Volterra filter," in Proc. IEEE ISCAS'00, vol. 5, pp. 249-252, May 2000.

[27] S. Kalluri and G. R. Arce, "A general calss of nonlinear normalized adaptive filtering algorithms," IEEE Tran. On Signal proc. Vol. 47 no 8, Aug. 1999.

[28] V. J. Mathews and G. L. Sicuranza, Polynomial Signal Processing, John Wiley & Sons, Inc. 2000.

[29] V. J. Mathews and J. Lee, "A fast recursive least squares second-order Vloterra filter," in Proc. IEEE Int. Conf. Acoustic, Speech, Signal Proc., pp. 1383-1386, 1988.

[30] A. Guerin, G. Faucon, and R. Le Bouquin-Jeannes, "Nonlinear acoustic echo cancellation based on Volterra filter," IEEE Trans. Speech Audio Process., vol. 11 no. 6, pp.672-683, Nov. 2003.

[31] A. Stenger and W. Kellermann, "Nonlinear acoustic echo cancellation with fast converging memoryless pre-processor," Proc. IEEE ICASSP'00, vol. 2, pp. 4.1805 - 4.1808, 5-9 June 2000.

[32] H. Dai and W. P. Zhu, "Compensation of Loudspeaker Nonlinearity in Acoustic Echo Cancellation Using Raised-Cosine Function," IEEE Trans. vol. 53, no. 11, pp. 1190 – 1194, Nov. 2006.

[33] T. Ogunfunmi and S. L. Chang, "Second-order adaptive Volterra system identification based on discrete nonlinear Wiener model," IEE proc. Vision, Image and Signal processing, vol. 148, no. 1, pp. 21-29, Feb. 2001.

[34] A. Fermo, A. Carini, and G. L. Sicuranza, "Simplified Volterra filters for acoustic echo cancellation in GSM receivers," in European Signal Process. Conf., Tampere, Finland, 2000.

[35] A. Fermo, A. Carini and G. L. Sicuranza, "Low-complexity nonlinear adaptive filters for acoustic echo cancellation in GSM handset receivers," Euro. Tans. Telecomms. 14:161-169, 2003.

[36] S. L. Chang and T. Ogunfunmi, "Performance analysis of nonlinear adaptive filter based on LMS algorithm," IEEE ACSSC'97, vol. 1, pp. 107-110, Nov. 1997.

[37] S.C. Douglas and T.H. Y. Meng, "An adaptive edge detection method using a modified sigmoid LMS algorithm", MAPLE PRESS pp:252-256, 1989.